Solid-State Structures of Metalloporphyrin NO_x Compounds

Graeme R. A. Wyllie and W. Robert Scheidt*

The Department of Chemistry and Biochemistry, University of Notre Dame, Notre Dame, Indiana 46556

Received July 10, 2001

Contents

I. Introduction 1067
A. Scope and Organization of the Review 1067
B. Coordination Modes for the NO_x Ligands and MNO_x Geometry 1068
C. Porphyrin Stereochemical Notation 1069
II. Nitrosyl Complexes 1070
A. "Miscellaneous" Nitrosyl Derivatives 1070
B. Group 8 Nitrosyls 1071
1. Iron Derivatives 1071
2. Ruthenium and Osmium Derivatives 1077
III. Nitrite and Nitrate Derivatives 1079
A. Nitrite Derivatives 1079
B. Nitrate Derivatives 1082
IV. Related Protein Structures 1083
A. $\{FeNO\}^7$ Proteins 1085
B. $\{FeNO\}^6$ Proteins 1086
C. Nitrite Binding Proteins 1086
V. Summary 1087
VI. Acknowledgments 1087
VII. Abbreviations 1087
A. Porphyrins and Ligands 1087
B. Proteins 1088
VIII. References and Notes 1088

I. Introduction

A. Scope and Organization of the Review

The interaction of metalloporphyrins with various nitrogen oxides of the general formula NO_x is of enormous physiological importance. Nitrosyl, nitrite, and nitrate metalloporphyrin complexes are involved in key processes in both the nitrogen cycle[1] and mammalian physiology, with examples of the latter including neurotransmission, vasodilation, and platelet aggregation.[2−4] The ability of nitric oxide to induce vasodilation and prevent blood clotting is also utilized by several species of insects that feed upon the blood of mammalian hosts.[5] An important issue is the interconversion of various nitrogen oxides in biology; both oxidation and reduction pathways are known. As the title suggests, we will primarily address structural aspects of the interaction of the nitrogen oxide ligands, nitric oxide, nitrite, and nitrate with metalloporphyrins.

* To whom correspondence should be addressed. E-mail: Scheidt.1@nd.edu. Fax: +(219) 631-4044.

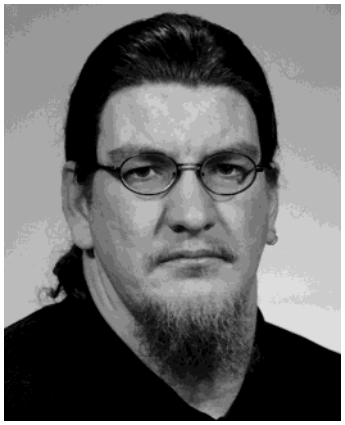

Graeme R. A. Wyllie is a graduate student at the University of Notre Dame currently working toward his Ph.D. He was born in Balloch, Scotland, and received his B.S. in chemistry from the University of St. Andrews working under the late Professor R. W. Hay. He completed a Postgraduate Diploma in Instrumental and Analytical Chemistry at Robert Gordon's University, Aberdeen, prior to joining Professor W. Robert Scheidt's group at Notre Dame. He is currently working on the interaction of NO_x ligands with metalloporphyrin systems.

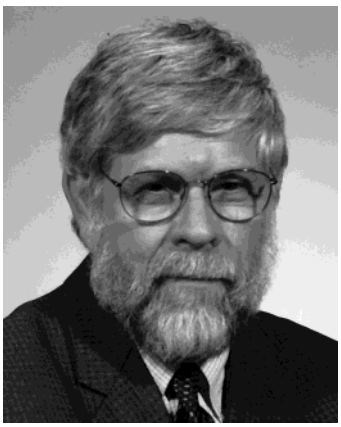

W. Robert Scheidt was born near St. Louis, MO. He received his B.S. in Chemistry from the University of Missouri–Columbia and his Ph.D. from the University of Michigan with Paul Rasmussen. After a postdoctoral stint with J. L. Hoard at Cornell University, he joined the Department of Chemistry and Biochemistry at the University of Notre Dame where he is now the Wm. K. Warren Professor.

A large volume of work has been published detailing the chemistry of nitrosyl complexes, including a number of reviews. Previous review articles have concentrated on matters such as structural aspects of both porphyrin and non-porphyrin complexes[6] and various aspects of the chemistry of nitrosyl-metalloporphyrin complexes[7,8] or have provided an overall coverage of the field of nitrosyl chemistry.[9] However, there has yet to be a review that examines the

10.1021/cr000080p CCC: $39.75
Published on Web 02/12/2002

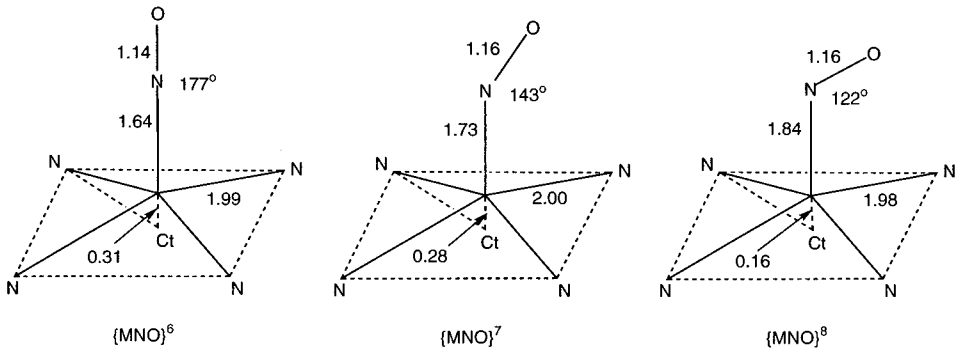

Figure 1. Formal diagrams for five-coordinate nitrosylmetalloporhyrin $\{MNO\}^n$ for $n = 6$, 7, and 8. Values for metrical parameters entered in the diagrams represent the author's estimates of the "best" geometry for each class.

structures of not only nitrosyl but also the related nitrite and nitrate metalloporphyrin complexes, and it is this role that this review intends to fulfill. The scope of this review is limited to metalloporphyrins and related macrocycles,[10] not only to provide a tighter focus but also to emphasize their physiological importance by comparing the structures of model complexes with the protein structures thus far obtained.

The purpose of this review is then to provide a comprehensive summary of existing metalloporphyrin NO_x structures and, where possible, carry out a correlation of the observed binding mode of the ligand with the relevant properties of the metalloporphyrin such as oxidation state, coordination environment, and electronic structure. Synthetic complexes for each of the three ligand types will be examined in turn starting with the nitrosyl complexes, which are the most numerous. We will divide the nitrosyl complexes into the iron triad of iron, ruthenium, and osmium, which we will denote as group 8, and the remainder, although it is to be recognized that group 8 is sometimes considered to contain a larger number of elements. This choice for group 8 metals serves to emphasize the biological importance of the iron-containing species. The remainder of nitrosyl complexes may sometimes be described as the "nongroup 8", a term that clearly lacks elegance in describing the remainder of the periodic table of nitrosyl-forming metalloporphyrins. The nitrite and nitrate examples will then be considered in turn. The review will then examine the existing protein structures that contain these coordinated ligands of the desired types. The binding modes of these will then be summarized and compared with the results obtained from the examination of the synthetic complexes in the previous sections.

B. Coordination Modes for the NO_x Ligands and MNO_x Geometry

The various metalloporphyrin $M(NO_x)$ complexes display a large number of possibilities in the binding of the NO_x ligand to the metal center. Variation can be observed in both the denticity and the identity of the atom(s) through which the ligand is coordinated. In this review, only those ligand bonding modes known or suspected in a metalloporphyrin system are considered; other possible bonding modes are generally disregarded. This latter category includes all bridging modes that are not relevant to the metalloporphyrin systems under review.

The most important coordination mode of nitric oxide is the N-bonded nitrosyl ligand. A great deal of early interest focused upon the observed M−N−O angle, which fell into one of two categories: linear or bent (∼120°). Early correlations of the observed M−N−O angle with the electronic structure tended to accentuate two distinct forms of the nitrosyl ligand: NO^+ and NO^-, which were associated with the linear and bent structures, respectively. However, this leads to problems in assigning the metal oxidation state, often giving formal oxidation states that are clearly unreasonable. Additionally, it is very difficult to predict what the observed M−N−O angle will be. The electron counting system of Enemark and Feltham[11] has provided more order in predicting MNO geometry. In this scheme, the MNO group is considered as a discrete entity; any assignment of the metal oxidation state is based upon the assumption that the NO ligand is a neutral species. Predictions of MNO geometry are then based on the number of electrons in the triatomic group and the overall geometry of the complex. For mononitrosyls, the number of electrons is the sum of metal d-electrons plus the electron in the π^* orbital of NO. This number of electrons (n) is expressed in the notation $\{MNO\}^n$. For nitrosylmetalloporphyrin systems, where the complexes are either five- or six-coordinate, and which possess square-pyramidal and pseudooctahedral geometries, respectively, the critical values of n in predicting geometry are found to be 6, 7, and 8. Limiting geometries are found at $n = 6$ and $n = 8$ where the M−N−O angles are approximately linear and strongly bent, respectively. Complexes possessing the intermediate value of n (7) are found to display intermediate M−N−O angles. Interestingly, the $n = 7$ case is observed only in derivatives with iron. To our knowledge, this is true no matter what the nature of the remaining ligands, porphyrin based or not. Following the above convention for assignment of oxidation state, all of the $\{FeNO\}^7$ derivatives are considered iron(II) species. The three cases, $n = 6$, 7, and 8, are schematically illustrated in Figure 1. Although the similarity between CO and linearly bound NO has sometimes been emphasized, there are significant differences as well between these diatomic ligands. We do not find the analogy to be particularly useful.

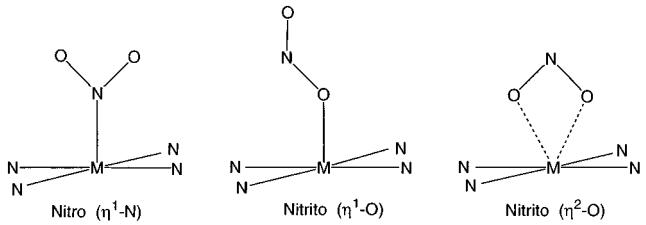

Figure 2. Schematic diagram illustrating the three limiting coordination modes of the nitrite ligand.

One other possible coordination mode for the nitrosyl ligand is η^1-O or isonitrosyl, where the nitrosyl is coordinated via the oxygen atom. Further details on this coordination mode can be found elsewhere in this issue.[12]

One last point concerning coordinated nitrosyls is that the nitrogen−oxygen bond length should show very little variation. This is true across the whole range of $\{MNO\}^x$ species, regardless of the degree of bending in the NO ligand. This is quite distinct from the behavior of, for example, coordinated dioxygen. Any difference in N−O bond lengths that results from electron donation or acceptance by the metal ion is likely to be as small or smaller than a number of other experimental effects. Three experimental effects that, in our judgment, could have significant effects on the experimentally determined N−O bond lengths are worthy of note: the effects of thermal motion, especially that of the nitrosyl oxygen atom, that will lead to a foreshortened calculated N−O bond length; the effect of positional disorder of the nitrosyl atoms that may be either major, that is, with well-separated atomic positions, or minor with effects leading to a thermal motion of the atoms that is apparently too large; and the effect of the presence of impurities near the position of the coordinated nitrosyl that might result from incomplete reaction. For example, the presence of a chloride or bromide impurity will place "ambiguous" electron density in the same region as the nitrogen and oxygen atoms of NO and affect the least-squares calculated atomic position of both atoms. Even relatively small amounts of such an impurity can have serious effects on either or both of the M−N or N−O bond lengths. In our view, the magnitude of the N−O bond length can be used as an internal check or quality marker for a particular structure. Unless a reasonable explanation is provided for the deviation, nitrosyl systems for which the N−O bond length shows significant variation from an expected range of 1.14−1.16 Å must be regarded with some caution. The degree of caution, of course, depends on the conclusions being reached; general geometric features are unlikely to be in error for modest deviations but may indeed be a concern for systems showing larger variation. The use of such questionable structures for subtle structural comparisons is likely to be of limited or no value. It is worth noting that this variation criterion raises a caution flag for more than half of the reported nitrosyl structures.

Significant variation is observed in the ligating atoms in coordinated nitrite systems. The three possibilities are shown in Figure 2. In the N-bound, or nitro case, the ligand is coordinated via the nitrogen atom. However, in the O-bound, or nitrito case, the ligand coordinates via either one or two oxygen atoms yielding η^1-O and η^2-O species. The nitrito and nitro systems can be discriminated from the symmetric and asymmetric stretches in the infrared. Both bands are very close in energy for the nitro system, while they are more widely spaced in the nitrito systems.

Although nitrate is a rather weakly coordinating anion, a few examples of metalloporphyrin nitrates have been structurally characterized. For the known nitrate systems, coordination is exclusively through oxygen atom(s); interesting variation occurs in the denticity of the ligand with the two limiting cases being mono- or bidentate coordination. There are also species that are readily described as intermediate to these limiting cases.

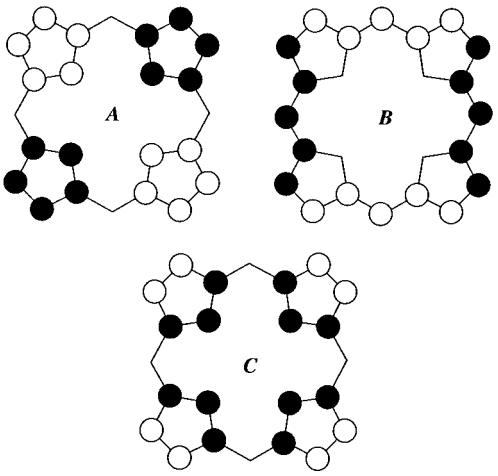

Figure 3. Schematic representations of three out-of-plane distortions found in metalloporphyrin species. The three modes shown are (A) saddling, (B) ruffling, and (C) doming. The filled and open circles represent atoms with displacements above and below the porphyrin mean plane, respectively. Atom positions with no circle are on the mean porphyrin plane.

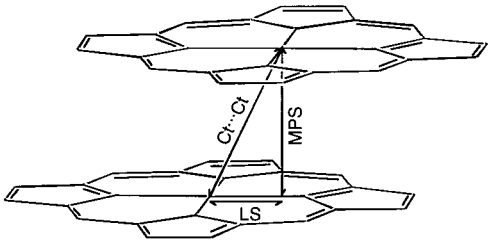

Figure 4. Illustration defining the mean plane separation (MPS), lateral shift (LS), and center to center (Ct···Ct) distances between a pair of closely interacting porphyrin rings.

C. Porphyrin Stereochemical Notation

We briefly note aspects of porphyrin stereochemical notation. In Figure 3, we display the pattern of deviations of the porphyrin core atoms from planarity. It is important to note that deformations perpendicular to the core are relatively low-energy distortions. Figure 4 illustrates some geometrical terms relating to the parameters used to describe a pair of closely interacting porphyrin rings, sometimes called $\pi-\pi$ interacting dimers.

Table 1. Summary of Coordination Group Geometry for Nongroup 8 Nitrosyl Metalloporphyrin Derivatives

complex	M−N_p[a]	M−N_{NO}[a]	∠MNO[b]	N−O[a]	Δ[a,c]	ν(NO)[d]	ref
[Co(TPP)(NO)][e]	1.978(4)	1.833(53)	∼135	1.01(2)	0.09	1689[f]	13
[Co(Tp-OCH_3PP)(NO)][g]	1.972(8)	1.855(6)	120.6(5)	1.159(8)	0.20	1696[f]	15
[Co(OEP)(NO)]	1.984(8) {1.9915(30), 1.9774(1)}[i]	1.844(9)	122.70(8)	1.1642(13)	0.16	1677[h]	16
[Co(OEP)(NO)]	1.985(2) {1.9925, 1.9780}[i]	1.844(2)	123.4(2)	1.152(3)	0.16	1675[f]	17
[Co(OEP)-*t*-Bu_2)(NO)][g]	1.949(9)	1.842(5)	124.7(5)	1.113(6)[j]	0.10		18
[Co(TPPBr_4NO_2)(NO)][k]	1.945(12)	1.827(21)	124.7(23)[l]	1.081(43)[l]	0.21	1710[m]	19
[Co(OC_2OPor)(NO)]	1.965(1)	1.837(4)	121.8(3)	1.174(4)	0.16	1667[f]	20
[Mn(TPP)(NO)(4-MePip)]	2.004(5)	1.641(2)	177.8(3)	1.160(3)	0.40	1735[f]	22, 21
[Mn(TTP)(NO)]	2.027(3)	1.644(5)	176.2(5)	1.176(7)	0.08	1740[f]	21
[Mo(TTP)$(NO)_2$]	2.165(9) {2.194(8), 2.135(8)}[p]	1.70(1)	158.0(8)	1.241	0.99	1600[n,o]	23
[Mo(TTP)(NO)(MeOH)]	2.091(4)	1.746(6)	179.8(4)	1.217	0.28	1540[n]	23

[a] Value in Å. [b] Value in deg. [c] Displacement of the metal atom out of the 24-atom porphyrin plane toward the nitrosyl group. [d] Value in cm^{-1}. [e] 8-Fold disorder of NO. [f] KBr pellet. [g] 2-Fold disorder of NO. [h] Nujol mull. [i] Long and short equatorial distances related to off-axis tilt of NO. [j] Value after correction for thermal foreshortening is 1.177(7) Å. [k] Packing disorder. [l] Average of two disordered positions. [m] $CHCl_3$ solution. [n] Benzene solution. [o] Two values of ν(NO) observed for dinitrosyl complex. [p] Long and short equatorial distances related to eclipse of nitrosyl with equatorial Mo−N_p bond.

II. Nitrosyl Complexes

A. "Miscellaneous" Nitrosyl Derivatives

Members of the "miscellaneous" nitrosyl derivatives are found on either side of the group 8 species (Fe, Ru, Os) in the periodic table. The nongroup 8 complexes are found to display a wide disparity in structural behavior and will provide an interesting backdrop against which to compare the structures of the group 8 complexes. The uniqueness of the iron porphyrinate derivatives is especially apparent when considered in this fashion.

By far, the most significant nongroup 8 metal that forms nitrosylmetalloporphyrin complexes is cobalt, both in terms of historical importance and in the number of structures reported. The five-coordinate complex [Co(TPP)(NO)] reported in 1973 by Scheidt and Hoard[13] was the first reported structure of a metalloporphyrin containing a coordinated nitrosyl group. This square-pyramidal {MNO}[8] complex displays a bent MNO geometry with a bond angle of ∼135°. This angle is somewhat larger than expected; values near 120° were found for several subsequent cobalt systems. The value of the angle is undoubtedly affected by the fact that the nitrosyl group is found to be crystallographically disordered over eight positions, a situation that corresponds to the appropriately named "Hydra Model" (Figure 5). An interesting question about the observed crystallographic disorder is whether the disorder reflects a real property of the molecules in the solid state. Otherwise put, is the observed crystalline disorder the result of random packing in the lattice (of molecules that differ in orientation of the nitrosyl, i.e., static disorder), or is the disorder a dynamic, solid-state process? ^{15}N CPMAS NMR spectroscopic studies by Mason[14] on [Co(TPP)(^{15}NO)] have shown that in the solid state above 200 K, the nitrosyl undergoes some kind of motion; this is determined to be either spinning or swinging. [Co(OEP)(^{15}NO)], which has a tightly packed, single-site NO position, does not show such behavior. This supports the idea that the NO disorder observed, predominantly for the tetraaryl systems, is a dynamic, solid-state process.

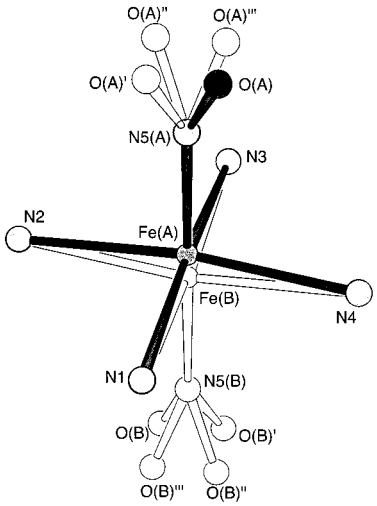

Figure 5. Diagram illustrating the 8-fold disorder of the MNO group in the five-coordinate derivatives [Co(TPP)(NO)] and [Fe(TPP)(NO)], the so-called "Hydra Model". The 8-fold disorder is a crystallographic symmetry requirement. One possible nitrosyl orientation is shown as shaded atoms, the other possible orientations are left unshaded but labeled.

The structural data for several other five-coordinate (nitrosyl)cobalt porphyrinate complexes have been reported and are summarized in Table 1.[15−20] The Co−N−O bond angles are all very similar over the range of complexes, while bond lengths for both Co−N(NO) and Co−N_p are also very comparable. The cobalt lies out of the porphyrin plane, toward the nitrosyl ligand, by an equivalent amount for each complex. Because the problem of ligand disorder is so prominent in structural nitrosyl chemistry, all structures known to be disordered have been identified in Table 1 and all subsequent tables. It is also worth noting that only five-coordinate square-pyramidal complexes have been reported for cobalt porphyrinates; a six-coordinate cobalt system containing a coordinated nitrosyl has yet to be found.

One noteworthy example is the structure of [Co(OEP)(NO)] reported by Ellison and Scheidt,[16] the molecular diagram of which is shown in Figure 6. This structure is of particular interest due to both

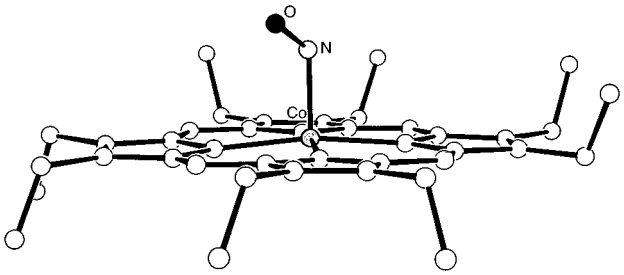

Figure 6. Molecular diagram of [Co(OEP)(NO)]. The 4-up, 4-down configuration of the peripheral ethyl group of the porphyrin is a common pattern in octaethylporphyrin complexes. Drawn from the coordinates reported in reference 16.

the off-axis tilt displayed by the Co−N(NO) bond vector and the asymmetry in the Co−N_p bonds. The latter is reflected in two inequivalent pairs of Co−N_p bonds with lengths of 1.977(1) and 1.992(3) Å, respectively, with the shorter bonds lying in the direction of the nitrosyl vector. The value of this off-axis tilt is found to be 2.2°, substantially less than that observed for similar iron systems, which are discussed below. A similar structural result was subsequently obtained by Godbout et al.[17]

One other structure of note is the capped porphyrin complex [Co(OC_2OPor)(NO)] system reported by Jene and Ibers.[20] The geometry of the CoNO unit is comparable to other nitrosyl cobalt porphyrins; the structure is notable for the coordination of the nitrosyl group on the exposed face of the porphyrin.

Apart from cobalt and the group 8 metals, two other nitrosylmetalloporphyrin systems have been structurally characterized: those formed from manganese and molybdenum porphyrinates. Five- and six-coordinate (nitrosyl)manganese porphyrinates have been prepared. These are {MnNO}^{6} systems; both a five-coordinate ([Mn(TTP)(NO)][21]) and a six-coordinate ([Mn(TPP)(NO)(4-MePip)][22]) species have been characterized. Both derivatives are found to possess nearly linear Mn−N−O units. The Mn−N(NO) bond is very short (1.64 Å) in both species; the bond trans to NO in the six-coordinate species is that expected for a low-spin manganese(II) porphyrin derivative. Complete data for the manganese complexes can be found in Table 1.

The molybdenum system is particularly intriguing since, under the correct experimental conditions, both mono- and dinitrosyl complexes have been isolated.[23] The six-coordinate mononitrosyl complex [Mo(TTP)(NO)(MeOH)] has the nitrosyl and methanol groups coordinated trans to each other with an out-of-plane Mo displacement of 0.28 Å toward NO, and an Mo−N−O angle of 179.8(4)°. The dinitrosyl complex, [Mo(TTP)$(NO)_2$] (Figure 7), surprisingly shows both nitrosyl groups coordinated on the same side of the porphyrin, consistent with the very large (0.99 Å) out-of-plane displacement of the metal. The average Mo−N−O bond angle is found to be 158.0(8)°, and the nitrosyl groups are found to be tilted toward each other with a N−Mo−N angle of 78.4(5)°. Even more amazingly, the O−Mo−O angle of 60.0(3)° shows that the oxygen atoms are tilted toward each other as well, so that the two NO ligands are in an "attracto" configuration. A cis-coordination mode is also observed for the dicarbonyl complex [Mo(TTP)$(CO)_2$].[24] In this case, the molybdenum−carbonyl group is linear; the angle at the molybdenum, C−Mo−C, is smaller at 66.3°, and there is not an attracto interaction between the two oxygen atoms. The molybdenum out-of-plane displacement is also smaller at 0.62 Å. This may be related to the fact that in the dicarbonyl complex, the axial ligands lie between a pair of Mo−N_p bonds, while in the dinitrosyl complex, the ligands are eclipsed with a pair of Mo−N_p bonds and the molybdenum is displaced further from the porphyrin plane to minimize steric interactions.

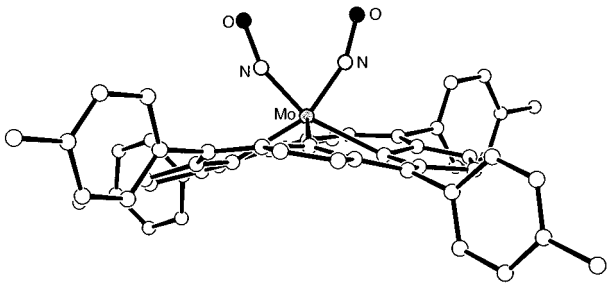

Figure 7. Molecular diagram of the molybdenum dinitrosyl species [Mo(TTP)$(NO)_2$]. This diagram illustrates the *attracto* or "rabbit ears" configuration taken up by the two nitrosyl ligands. Drawn from coordinates reported in ref 23.

B. Group 8 Nitrosyls

1. Iron Derivatives

The (nitrosyl)iron porphyrinate complexes are conveniently divided into {FeNO}^{7} and {FeNO}^{6} systems. Following the convention that NO is always considered a neutral species, these systems can also be assigned as formal iron(II) and iron(III) systems, respectively. The more numerous {FeNO}^{7} species were also those initially characterized.

Five-Coordinate {FeNO}^{7} Species. The first system reported was five-coordinate [Fe(TPP)(NO)][25] in 1975. Like the [Co(TPP)(NO)] system, the nitrosyl group is highly disordered over eight distinct positions. The value of the Fe−N−O angle (149.2(6)°) lies between that observed for the strongly bent {CoNO}^{8} cobalt systems and the linear {MnNO}^{6} systems. Although the canonical Fe−N−O value is likely to be a bit smaller than the 149° value found here, the Fe−N−O angle for these {FeNO}^{7} systems is clearly intermediate and unique. The structures of several additional five-coordinate complexes, formed with other tetraarylporphyrin ligands, have been subsequently reported. With one notable exception, these tetraarylporphyrin derivatives also suffer from disorder that severely limits their metrical utility with respect to details for Fe−N−O bonding. It appears that the aryl groups are bulky enough to form ligand binding pockets in the solid state that allow for two or more orientations of the bent nitrosyl group, with or without required crystallographic symmetry. This observation suggests that the barrier to rotation around the Fe−N(NO) bond is relatively low, although to our knowledge, there is no quantitative data on the issue.

Though there are a number of disordered structures, there have also been, quite recently, several

Table 2. Summary of Coordination Group Geometry for Five-Coordinate (Nitrosyl)Iron(II) Metalloporphyrin Derivatives

complex	Fe−N_p[a]	Fe−N_{NO}[a]	∠FeNO[b]	N−O[a]	Δ[a,c]	ν(NO)[d]	ref
[Fe(TPP)(NO)][e]	2.001(3)	1.717(7)	149.2(6)	1.122(12)	0.211	1670[f]	25
[Fe(TPPBr_8)(NO)][g]	1.986(23)	1.75(6)	146(2)	1.42(7)		1685[f]	31
[Fe(T2,6-Cl_2PP)(NO)][h]	2.00	1.70(1)	138.8(9)			1688[f]	31
[Fe(TpivPP)(NO)][i]	1.981(26)	1.716(15)	143.8(17)	1.197(9)	0.27	1665[f]	29
[Fe(TpivPP)(NO)][j,k]	1.99−2.01	1.65(5)	149(4)	1.17(5)		1675[f]	30
		1.74(6)[l]	137(4)[l]	1.20(7)[l]			
[Fe(TPPBr_4)(NO)](B)[m]	1.951(35)	1.691(11)	145(1)	1.145(16)	0.29	1681[n]	27
[Fe(TPPBr_4)(NO)](A′)[o]	2.006(35) {2.041(9), 2.031(8)}[p]	1.734(8)	147.9(8)	1.119(111)	0.27	1678[n]	27
[Fe(TPPBr_4)(NO)](A″)[o]	1.996(24) {2.027(7), 2.004(7)}[p]	1.726(9)	146.9(9)	1.144(12)	0.32	1678[n]	27
[Fe(OEP)(NO)](A)[q]	2.004(15) {2.016(1), 1.991(3)}[p]	1.722(2)	144.4(2)	1.167(3)	0.29	1666[n]	26, 27
[Fe(OEP)(NO)](B)[r]	2.010(130 {2.020(4), 1.999(1)}[p]	1.7307(7)	142.74(8)	1.1677(11)	0.27	1673[n]	26, 27
[Fe(OETAP)(NO)]	1.931(9) {1.940(2), 1.924(2)}[p]	1.721(4)	143.7(4)	1.155(5)	0.31	1666[f]	28
[Fe(oxoOEC)(NO)]	2.009(9)	1.7320(13)	143.11(15)	1.1696(19)	0.26	1690[n]	27

[a] Value in Å. [b] Value in deg. [c] Displacement of the metal atom out of the 24-atom porphyrin plane toward the nitrosyl group. [d] Value in cm^{-1}. [e] 8-Fold disorder of NO. [f] KBr pellet. [g] 4-Fold disorder of NO. [h] Incomplete structure reported; severe disorder? [i] Two positions observed for nitrosyl ligand. [j] Two positions of nitrosyl. [k] Severe disorder. [l] Second disordered position of nitrosyl, still within pocket. [m] Ruffled form, 2-fold disordered. [n] Nujol mull. [o] Saddled forms, two independent molecules. [p] Long and short equatorial distances, relating to off-axis tilt of NO. [q] Monoclinic form. [r] Triclinic form.

well-ordered and highly precise five-coordinate structures reported.[26−28] Data for all of the iron(II) systems are listed in Table 2.[25−31] An examination of these data suggests that the axial Fe−N(NO) bond length is constant at 1.72−1.73 Å. The value of the Fe−N−O angle from the well-ordered structures suggests that the value is in the 143−144° range. The data of Table 2 show that the iron atom is displaced toward nitric oxide by a bit less than 0.3 Å. A comparison of the corresponding values for the $\{CoNO\}^8$ and $\{MnNO\}^6$ species (Table 1) shows that the values observed for the iron species are again intermediate to those seen in what we regard as the limiting cases. The variation in the M−N(NO) bond distance reflects the difference in axial bonding; the linear case has one σ and two M−N π bonds, while one π interaction is gradually lost in the transition to the strongly bent Co system. The differences in metal ion displacement in the five-coordinate complexes, which are in the order Co < Fe < Mn, reflect the nonbonding interactions between the pyrrolic nitrogens of the porphyrin core and the nitrogen atom of the nitrosyl. That the nonbonded interactions remain roughly constant is seen by the fact that the nitrosyl nitrogen to porphyrin core center distance remains almost constant at ∼2.0 Å in all derivatives. (This is the sum of the displacement of the metal plus the M−N(NO) bond distance in Figure 1.)

The equatorial Fe−N_p bond length of 2.001(3) Å found in [Fe(TPP)(NO)] is typical for a low-spin iron(II) center.[32] The variation observed (1.98−2.01 Å) in all of the iron(II) systems (summarized in Table 2) reflects core conformation differences.

Recent structure determinations of ordered five-coordinate iron(II) derivatives led to the recognition of interesting distortions that appear to be intrinsic features of the total Fe−NO bonding interactions in the complexes. This effect was first described for two distinct crystalline forms of [Fe(OEP)(NO)].[26] The nitrosyl group in both OEP derivatives is completely

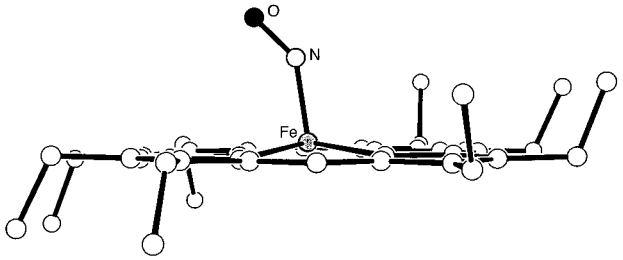

Figure 8. Molecular diagram of [Fe(OEP)(NO)]. The off-axis tilt of the Fe−N−O moiety is clearly visible. Drawn from coordinates reported in refs 26 and 27.

ordered. Structural features of one derivative are illustrated in Figure 8; the features of the other derivative are comparable. The first structural distortion feature was a significant tilting of the axial Fe−N(NO) bond from the porphyrin plane normal. The magnitude of this off-axis tilt has the Fe−N vector lying off the heme normal by 8.2°, which results in the displacement of the nitrosyl nitrogen by 0.25 Å from the heme normal. The second structural distortion is the appearance of longer and shorter Fe−N_p bond distances in a pattern that is related to the orientation of the bent and tilted FeNO group. In the [Fe(OEP)(NO)] derivatives, the two Fe−N_p bonds along the Fe−N(NO) bond-tilt direction are shortened, while the two other Fe−N_p bonds, away from the bond-tilt direction, are lengthened. Although the distance changes are small (Δ(Fe−N_p) ≈ 0.025 Å) and the tilt of the Fe−N vector off the heme normal is also small (tilt ≈ 6−8°), the high quality of the two [Fe(OEP)(NO)] structures leads to statistically significant differences in the two sets of equatorial bonds.

As can be noted in Figure 8, the ordered nitrosyl group is oriented opposite the four face-up ethyl groups. However, the orientation of the NO appears totally unrelated to the orientation of the ethyl groups, as the intramolecular distances between the two groups are relatively large. Rather, the four-up,

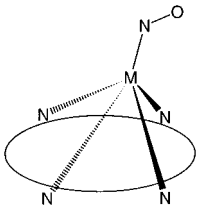

Figure 9. Formal diagram illustrating the tilt/asymmetry found in the ordered five-coordinate [Fe(Por)(NO)] derivatives. All distortions have been exaggerated for clarity.

four-down ethyl group pattern is the result of a modest $\pi-\pi$ interaction between pairs of OEP rings. Both the [Fe(OEP)(NO)] derivatives form class I dimers in the solid state. Such $\pi-\pi$ interactions were described earlier by Scheidt and Lee.[33]

Figure 9 schematically (and exaggeratedly) shows the pattern of Fe−N_p bond distance changes observed in the (nitrosyl)(porphinato)iron(II) derivatives. Additional ordered derivatives support the idea that this tilt/asymmetry is a general effect. An oxochlorin derivative, [Fe(oxoOEC)(NO)], related to the d_1 heme of the cd_1 dissimilatory nitrite reductase, shows a similar tilt/asymmetry pattern. Iron(II) nitrosyl derivatives with $TPPBr_4$ display two distinctly different saddled conformations in which the NO group tilts toward one of the trans-brominated pyrroles. Moreover, Bohle et al.[28] have reported the structure of five-coordinate [Fe(OETAP)(NO)], where the same tilt/asymmetry pattern is present. The pattern is thus present in all ordered five-coordinate iron(II) species. That the same effects, with a smaller magnitude, are seen in two independent structure determinations of [Co(OEP)(NO)][16,17] suggests an electronic basis for the tilt/asymmetry. A qualitative molecular orbital picture has been used to rationalize the tilt/asymmetry in the M−N−O geometry.[27] Two different sets of density functional theory (DFT) calculations support the effect as being intrinsic to the bonding, although the full details are somewhat different.[34,35] It is yet to be determined whether this tilting leads to any particular reactivity, but the characteristic tilting is consistent with the FeNO unit dominating the bonding in the complexes.

Six-Coordinate {FeNO}^{7} Species. For reasons that will become evident, there are relatively few structurally characterized six-coordinate examples of {FeNO}^{7} derivatives. The structure of the first of these, [Fe(TPP)(NO)(1-MeIm)],[22,36] demonstrated two important features. First, any changes in the coordination parameters of the FeNO group upon the increase in coordination number are nonexistent or very small. This includes both the Fe−N−O angle and the Fe−N(NO) bond length. Second, the nitrosyl group exhibits a strong structural trans effect. The Fe−N(MeIm) bond length of 2.180(4) Å is noted as being particularly long compared to the less than 2.00 Å value typically seen for six-coordinate bis(imidazole) iron(II) species.[37] Related six-coordinate systems that utilize 4-methylpiperidine as the sixth ligand trans to NO have also been characterized.[38] This system had been chosen to provide a ligand with somewhat differing (greater) steric requirements than that of the planar imidazole ligand. There are two crystalline forms of [Fe(TPP)(NO)(4-MePip)], and

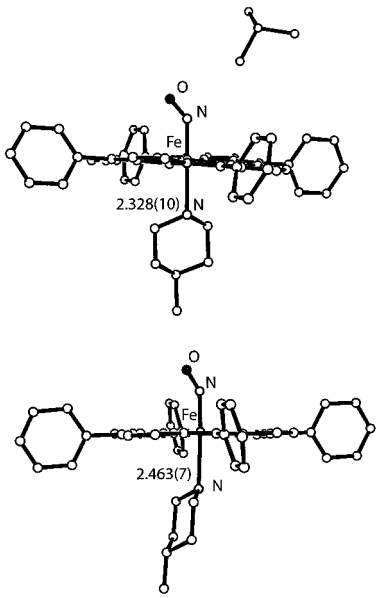

Figure 10. Molecular diagram representing the two crystalline forms of [Fe(TPP)(NO)(4-MePip)]. The solvated form is shown at the top and the unsolvated form at the bottom. Drawn from coordinates reported in ref 38.

each form has a significantly different value for the Fe−N(4-MePip) bond distance (2.328 and 2.463 Å). These two forms are illustrated in Figure 10. Both values are consistent with a structural trans effect that leads to a greater than 0.20 Å lengthening of the bond trans to NO.[39] The significant difference in the two observed Fe−N(4-MePip) bond distances suggests that the ready variability in the length of the bond trans to NO is due to an extremely weak bond. Exactly which electronic features play a role in the trans distance is not clear. However, the structural characterization of additional six-coordinate examples along with electronic structure characterization is in prospect.[40] Structural parameters for all known six-coordinate {FeNO}^{7} systems are given in Table 3.

The electronic basis for the structural trans effect is a partial population of the d_z^2 orbital by an unpaired electron derived from the nitrosyl ligand. Both Kon[41] and Wayland[42] demonstrated from the EPR spectra, which show hyperfine splitting from both axial nitrogen atoms, that this orbital must contain significant unpaired electron density. This orbital combination must be antibonding with respect to the binding of the sixth ligand. The structural trans effect in the {FeNO}^{7} systems leads to the very low binding constant values for the ligand trans to NO; estimates range from 0.1 to 10. Such low values preclude the complete formation of a six-coordinate iron(II) system in solution.

The structural trans effect is apparently the mechanism by which NO acts as a messenger and turns on the enzyme guanylate cyclase.[43] NO as a signaling agent coordinates to a five-coordinate histidine-ligated heme; the consequent NO trans effect leads to a breaking of the trans iron−histidine bond.[43] A proposed conformational change of the multiunit protein then leads to activity. An unexpected feature of the enzyme is the selective binding of NO; the

Table 3. Summary of Coordination Group Geometry for Six-Coordinate (Nitrosyl)Iron(II) Metalloporphyrin Derivatives

complex	Fe−N_p[a]	Fe−N_{NO}[a]	∠FeNO[b]	N−O[a]	Δ[a,c]	Fe−L[a]	ν(NO)[d]	ref
[Fe(TPP)(NO)(1-MeIm)][e]	2.008(12)	1.743(4)	142.1(6)	1.121(8)	0.07	2.180(4)	1625[f]	22, 36
[Fe(TPP)(NO)(4-MePip)](form 1)[c,g]	2.004(9)	1.7210(10)	138.5(11)	1.141(13)	0.09	2.328(10)	1640[f]	38
[Fe(TPP)(NO)(4-MePip)](form 2)[e]	1.998(10)	1.740(7)	143.7(6)	1.112(9)	0.11	2.463(7)	1653−1656[f]	38
[Fe(TPP)(NO)(NO_2)][h,i]	1.988(6)	1.792(8)	137.4(6)	1.176(8)	0.10	2.086(8)	1616[e]	49
[Fe(TPP)(NO)(NO_2)][j]	1.986(6)	1.840(6)	137.4(6)	1.134(8)	0.09	2.060(7)	1668[k]	49

[a] Value in Å. [b] Value in deg. [c] Displacement of the metal atom out of the 24-atom porphyrin plane toward the nitrosyl group. [d] Value in cm^{-1}. [e] Two positions of nitrosyl ligand observed. [f] KBr pellet. [g] Solvated form. [h] ⊥ form. [i] Two independent molecules, one disordered. [j] || form. [k] Nujol mull.

affinity for dioxygen is much lower.[44] The NO structural trans effect also leads to significant differences in the physical properties of (nitrosyl)hemoglobin in the presence of allosteric effectors. The investigation of the addition of inositol hexaphosphate to (nitrosyl)-hemoglobin by IR, RR, or EPR spectroscopy leads to the conclusion that some bond breakage must occur in one set of subunits.[45,46] Interestingly, phenomena that must center around the structural trans effect lead to the selective bonding of NO by the α subunits of hemoglobin.[47] Hemoglobin, when half-saturated with NO to form $\alpha(FeNO)_2\beta(Fe)_2$, still retains cooperative binding of O_2. This may have significance in the physiology of NO.

There are two distinct orientations of the bent FeNO unit in crystalline [Fe(TPP)(NO)(1-MeIm)], which probably reflects that the packing environment on the NO side of the porphyrin plane is relatively open. A consideration of the possibility of metal−ligand π bonding for the two axial ligands suggests that the dihedral angle between the imidazole plane and the Fe−N−O plane should be either ∼90 or ∼0°, that is, either a relative perpendicular or parallel orientation. Imidazole is expected to be a modest π donor, while NO is expected to be strongly π accepting, hence an angle of near 0° might be predicted since this would maximize the synergic effects of the π bonding of the system. The observed dihedral angles, 21° for the major NO orientation and 36° for the minor NO orientation, are consistent with some degree of synergic π bonding.

The issue of π-bonding synergism also arises in a rather novel six-coordinate system, [Fe(TpivPP)(NO)-(NO_2)]$^-$, where both axial ligands should be considered as strong π acceptors. As a result, the nitrosyl might no longer solely dominate the bonding. The complex is formed by the addition of NO to the preformed anionic, low-spin species [Fe(TpivPP)-(NO_2)]$^-$.[48] Two distinct crystalline forms of [Fe-(TpivPP)(NO)(NO_2)] are observed that differ in the relative orientation of the nitrosyl and nitrite ligand planes.[49] The first form has the two ligand planes with an approximately perpendicular relative orientation, while the second crystalline form has both planes with a nearly parallel orientation (dihedral angle of 20.9°). The differences in relative orientation might be expected to be reflected in structural and electronic structure properties such as EPR, IR, and Mössbauer spectroscopy. Unfortunately, the molecular structures are not determined to a sufficiently high degree of precision to allow any statements concerning bond distance differences between the two types of structures. The IR and Mössbauer spectra

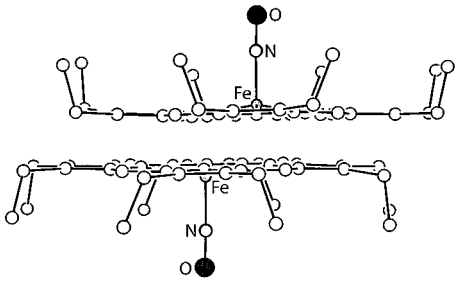

Figure 11. Molecular diagram of the observed π−π dimer for [Fe(OEP)(NO)]ClO_4·$CHCl_3$. The interplanar spacing of 3.3 Å is clearly apparent. Drawn from coordinates reported in ref 50.

of the form with relative perpendicular orientation of the two axial ligands resemble those of six-coordinate {FeNO}^{7} systems while the relative parallel form yields spectra similar to those seen for the five-coordinate nitrosyl species. Thus in the relative perpendicular form, the two ligands appear to equally compete for π electron density from two distinct dπ orbitals. However, in the relative parallel form, the two ligands do not seem to equally compete for π electron density from the same dπ orbital and NO appears to dominate the bonding.[48]

{FeNO}^{6} Species. The first structurally characterized {FeNO}^{6} complexes (iron(III)) were reported nearly 10 years after those of their iron(II) analogues. Difficulties in obtaining stable, isolable iron(III) species arise from the facile reduction of iron(III) by NO in a reductive nitrosylation reaction, a reaction more problematic for tetraaryl porphyrins. Solid-state {FeNO}^{6} species also readily effloresce NO on standing. The first two {FeNO}^{6} complexes characterized were six-coordinate [Fe(TPP)(NO)(OH_2)]ClO_4 and five-coordinate [Fe(OEP)(NO)]ClO_4·$CHCl_3$.[50] Both {FeNO}^{6} complexes display a linear FeNO unit in contrast to the bent {FeNO}^{7} moiety previously described. The Fe−N(NO) bond length is shorter at 1.64−1.65 Å, consistent with increased π bonding between iron and nitric oxide. The {FeNO}^{6} complexes are low spin, as expected, with bond distances comparable to other low-spin iron(III) systems.[32]

Five-coordinate [Fe(OEP)(NO)]ClO_4 has a structure typical of square-pyramidal species with the iron atom displaced 0.29 Å out of the porphyrin plane toward the nitrosyl group. The complex exhibits intermolecular interactions that result in the formation of a π−π dimer system as illustrated in Figure 11. The mean separation between the porphyrin planes is 3.3 Å, which falls within the characteristic range of π−π-interacting systems.[33] The two porphy-

Table 4. Summary of Coordination Group Geometry for (Nitrosyl)Iron(III) Metalloporphyrin Derivatives

complex	Fe−N_p[a]	Fe−N_{NO}[a]	∠FeNO[b]	N−O[a]	Δ[a,c]	Fe−L[a]	ν(NO)[d]	ref
[Fe(OEP)(NO)]ClO_4[e]	1.994(1)	1.644(3)	176.9(3)	1.112(4)	0.29		1868[f]	50
[Fe(OEP)(NO)]ClO_4[g]	1.994(5)	1.6528(13)	173.19(13)	1.140(2)	0.32		1838[h]	51
[Fe(OEP)(NO)(1-MeIm)]$^+$	2.003(5)	1.6465(17)	177.28(17)	1.135(2)	0.02	1.9889(16)	1921[h]	54
[Fe(OEP)(NO)(Pz)]$^+$	2.004(5)	1.627(2)	176.9(3)	1.141(3)	0.01	1.988(2)	1909[h]	54
[Fe(OEP)(NO)(Iz)]$^+$	1.996(4)	1.632(3)	177.6(3)	1.136(4)	0.04	2.010(3)	1914[h]	54
{[Fe(OEP)(NO)]$_2$Prz}$^{2+}$	1.995(8)	1.632(3)	176.5(3)	1.131(4)	0.06	2.039(2)	1899[h]	54
[Fe(TPP)(NO)(OH_2)]$^+$	1.999(6)	1.652(5)	174.4(10)	1.150	NA[i]	2.001(5)	1937[f]	50
[Fe(TPP)(NO)(HO-*i*-C_5H_{11})]$^+$	2.013(3)	1.776(5)	177.1(7)	0.925(6)	0.05[j]	2.063(3)	1935[f]	53
[Fe(TpivPP)(NO)(NO_2)][k]	2.000(5)	1.668(2)	180.0[l]	1.132(3)	0.15	2.002(2)	1893[h]	55
[Fe(TpivPP)(NO)(NO_2)]	1.996(4)	1.671(2)	169.3(2)	1.144(3)	0.09	1.998(2)	1893[h]	55
[Fe(OEP)(NO)(*p*-C_6H_4F)]	2.016(11)	1.728(2)	157.4(2)	1.153(3)	0.09	2.040(3)	1839[h]	56
[Fe(OECorrole)(NO)]$^+$	1.909(3)	1.631(3)	176.9(3)	1.171(4)	0.47[j]		1758[m]	52
[Fe(OECorrole$^•$)(NO)]$^+$	1.912(8)	1.655(10)	171.4(9)	1.115(12)	0.41[j]		1809[m]	52

[a] Value in Å. [b] Value in deg. [c] Displacement of the metal atom out of the 24-atom porphyrin plane. [d] Value in cm^{-1}. [e] Solvated form. [f] KBr Pellet. [g] Nonsolvated form. [h] Nujol mull. [i] Obscured by required crystallographic disorder. [j] Displacement of the metal atom from the mean plane of the four nitrogen atoms. [k] 2-Fold disorder of the nitrosyl ligand. [l] Required by crystallographic symmetry. [m] CsI pellet.

rin rings are laterally shifted by ∼1.43 Å, which results in a Ct···Ct distance of 3.652 Å and an Fe···Fe separation of 4.238 Å. These parameters are illustrated in Figure 4. The structure of the six-coordinate system, [Fe(TPP)(NO)(OH_2)]ClO_4,[50] although exhibiting some disorder in the two axial ligands, demonstrated that the effect of a sixth ligand on the FeNO group would be small. Subsequently, a number of other (nitrosyl)iron(III) porphyrinates (and a related corrole system) have been characterized.[50,51−56] The bonding parameters for all of these complexes are displayed in Table 4.

Included in these subsequently characterized species is a second crystalline form of [Fe(OEP)(NO)]ClO_4,[51] which differs from the first by the absence of a chloroform solvent molecule in the crystalline lattice. Quite surprisingly, the solid-state IR spectrum of this crystalline form displays a nitrosyl absorption band (ν(NO)) that differs from the original form by 30 cm^{-1} (1838 vs 1868 cm^{-1}). Differences in the two solid-state structures that could lead to the differing vibrational absorption spectra were sought but without a definite conclusion, although several possible causes were identified.[51] In this second crystalline form, π−π-interacting dimers were again observed with a porphyrin plane separation of 3.41 Å, an Fe···Fe distance of 4.24 Å, and a Ct···Ct distance of 3.65 Å. The lateral shift, 1.32 Å, is smaller but also differs from the previous structure by the direction in which this shift occurs. In the solvated form, the two porphyrins are shifted along the Fe−N_p bond, while in the nonsolvated form, this shift occurs at a direction of 45° to an Fe−N_p bond. This is illustrated in Figure 12. A similarly laterally shifted π−π dimer structure is observed for the iron(III) corrole system, [Fe(OECorrole)(NO)], although with a larger separation between the two corrole planes (3.6−3.7 Å) and a larger out-of-plane displacement of the iron (0.47 Å) that results in a large Fe···Fe separation of 6.32 Å. The FeNO unit is again linear, and bond lengths are comparable to the porphyrin systems. Oxidation of this species yields the ring-oxidized [Fe(OECorrole$^•$)(NO)]$^+$, which forms a tighter π−π dimer with an interplanar separation of only 3.21 Å and an Fe···Fe distance of 3.96 Å.

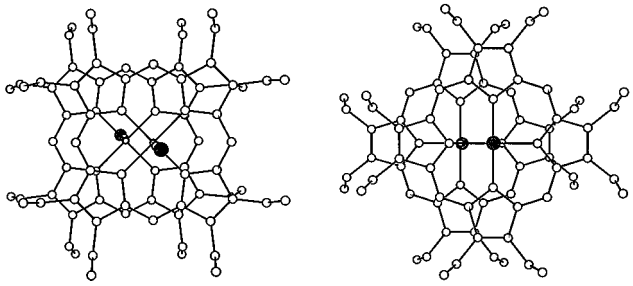

Figure 12. Direction of the lateral shifts for the two crystalline forms of the [Fe(OEP)(NO)]$^+$ species. The left-hand diagram is the $CHCl_3$ solvated form (ref 50), while the right-hand diagram is the unsolvated form (ref 51). Diagrams are based upon coordinates given in refs 50 and 51.

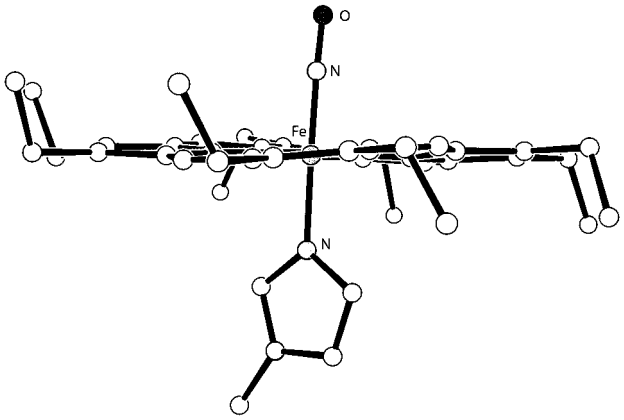

Figure 13. Molecular diagram of the {FeNO}^{6} complex [Fe(OEP)(NO)(1-MeIm)]$^+$. The Fe−N−O angle is 177.3(2)°, and the N−Fe−N angle is 178.8(1)°. Drawn from coordinates reported in ref 54.

A series of six-coordinate complexes, [Fe(OEP)(NO)(L)]ClO_4, where L is a neutral nitrogen donor ligand, have also been prepared and characterized.[54] One of these complexes, [Fe(OEP)(NO)(1-MeIm)]$^+$, is illustrated in Figure 13. In general, the geometry of the FeNO group upon addition of a trans (sixth) ligand does not change. Indeed, perhaps counterintuitively, if there is any difference in the Fe−N(NO) bond length, it becomes slightly shorter upon coordination of the sixth ligand. In the six-coordinate species, however, the iron is located close to the

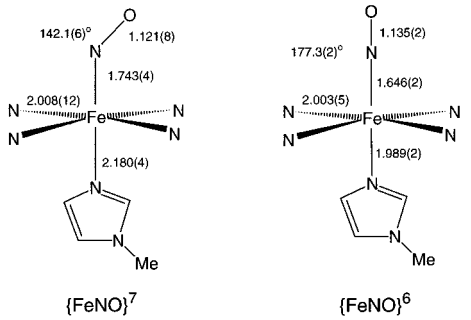

Figure 14. Comparison of structural parameters for six-coordinate $\{FeNO\}^7$ and $\{FeNO\}^6$ complexes. Values for the structures of [Fe(TPP)(NO)(1-MeIm)] and $[Fe(OEP)(NO)(1\text{-MeIm})]^+$ are taken from refs 36 and 54, respectively. 1-Methylimidazole ligands are displayed with arbitrary orientations.

center of the porphyrin plane. Thus, the nitrosyl nitrogen atom is correspondingly closer to the porphyrin plane than in the five-coordinate species; a slight reverse doming of the porphyrin core is observed for all of these six-coordinated systems. In addition to this reverse doming, ruffling or saddling of the porphyrin core is also observed for all structures leading to an overall picture of a porphyrin core more distorted than that in either the five-coordinate iron(III) or iron(II) systems. One of the most important results, however, is the observation that the (trans) bond lengths for the Fe−N(L) bond are comparable to those of other low-spin iron(III) systems, demonstrating that the nitrosyl group does not display a trans effect in the iron(III) systems. Moreover, within very tight experimental uncertainties, the effect of various types of trans nitrogen donors on the FeNO geometry is also negligible. A comparison of the bonding parameters for the iron(II) and iron(III) $[Fe(por)(NO)(1\text{-MeIm})]^{0/+}$systems is shown in Figure 14.

The significantly shorter Fe−N(NO) bond distance in the $\{FeNO\}^6$ species clearly leads to the notion that this bond is significantly stronger in $\{FeNO\}^6$ than in the $\{FeNO\}^7$ complexes. Nonetheless, the NO binding constant is much larger for the $\{FeNO\}^7$ species[57] ($\sim 10^{11}$ compared to a binding constant of 10^3-10^5 for the $\{FeNO\}^6$ species[58]). Much, but not all, of the difference in binding constants is a reflection of the greater lability (k_{off}) of NO in the $\{FeNO\}^6$ systems.

Since the addition of excess quantities of the neutral ligand results in formation of the $[Fe(OEP)(L)_2]^+$ species, most of these complexes are synthesized using limited quantities of the sixth ligand. Under certain conditions, the addition of pyrazine to $[Fe(OEP)(NO)]ClO_4$ leads to an interesting binuclear species illustrated in Figure 15. This complex, $\{[Fe(OEP)(NO)]_2(Prz)\}(ClO_4)_2$,[54] consists of the two iron porphyrins linked by a bridging pyrazine group. Compared to the mononuclear $[Fe(OEP)(NO)(Prz)]ClO_4$, the iron is displaced more out-of-plane toward NO (by ~0.05 Å) and the Fe−N(Prz) bond is longer for the binuclear species. Apart from these, all bonding parameters are equivalent. An interesting argument is given in this paper for correlating infrared stretching frequency with intermolecular

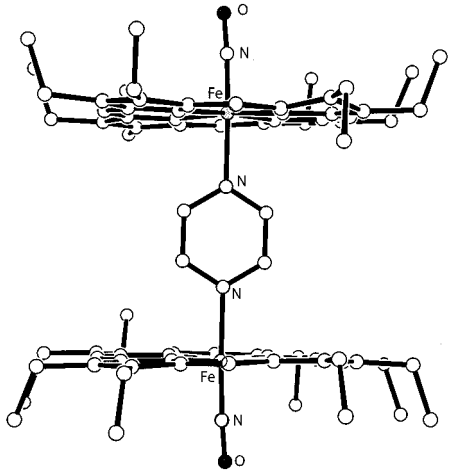

Figure 15. Molecular diagram of the binuclear complex $\{[Fe(OEP)(NO)]_2(Prz)\}$. Drawn from coordinates reported in ref 54.

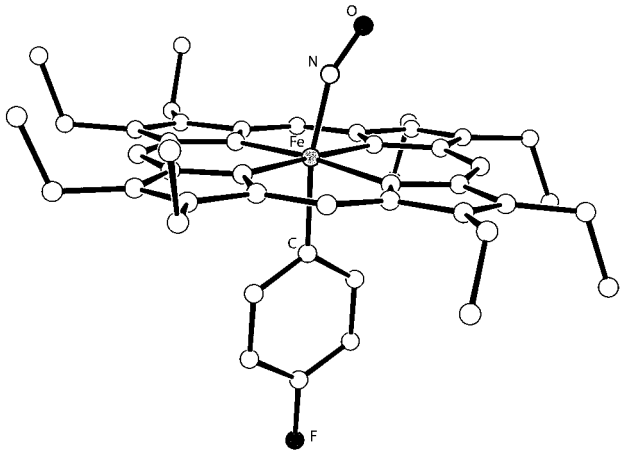

Figure 16. Molecular diagram of $[Fe(OEP)(NO)(p\text{-}C_6H_5F)]$. Drawn from coordinates reported in ref 56.

interactions. The intermolecular interactions lead to changes of $\sim 15-25$ cm^{-1} in frequency. The range of nitrosyl frequencies in these neutral nitrogen species is $1921-1890$ cm^{-1}. Interested readers are advised to consult the original paper.[54]

The structure of $[Fe(OEP)(NO)(p\text{-}C_6H_4F)]$ demonstrates an important issue for $\{MNO\}^6$ species, namely, that the ligand trans to NO can have a profound effect on the MNO geometry.[56] The FeNO group in this complex is strongly bent, not linear, with an Fe−N−O angle of 157.4°, but that angle is clearly larger than those of $\{FeNO\}^7$ species. The longer Fe−N(NO) bond distance and an apparent elongation of the trans Fe−C bond are other features that are atypical of other iron(III) systems. The molecular diagram of this complex is shown in Figure 16. Applied magnetic field Mössbauer spectroscopy for $[Fe(OEP)(NO)(p\text{-}C_6H_4F)]$ clearly demonstrates diamagnetism for the complex, and hence the assignment as $\{FeNO\}^6$ is incontrovertible. $\{FeNO\}^6$ nitrosyl derivatives with strongly σ-bonding alkyl and aryl groups trans to NO are known to have anomalously low nitrosyl stretching frequencies.[59] This result, along with the structural results for similar ruthenium systems (vide infra), is strong evidence for unique structural properties for derivatives that

Table 5. Summary of Coordination Group Geometry for (Nitrosyl)Ruthenium Metalloporphyrin Derivatives

complex	Ru−N_p[a]	Ru−N_{NO}[a]	∠RuNO[b]	N−O[a]	Δ[a,c]	Ru−L[a]	ν(NO)[d]	ref
[Ru(TTP)(NO)(OMe)][e]	2.050(3)	1.84(4)	180.0[f]		0.0[g]	1.80(5)	1800[h]	64
[Ru(OEP)(NO)(OH_2)]$^{+}$ [e]	2.041(4)	1.888(5)[i]	171.0(7)	1.138(12)	0.0[g]	1.888(5)[i]	1853[h]	65
[Ru(OEP)(NO)(OH)]	2.060(3)	1.723(11)	173.7(12)	1.155(14)		1.956(11)	1806[h]	69
[Ru(TPP)(NO)(OH)][j]	2.050(4)	1.726(9)	180.0[f]	1.170(9)	0.0[g]	1.873(11)	1827[h]	69
[Ru(TTP)(NO)(OH)]	2.055(5)	1.751(5)	167.4(6)	1.142(8)	0.05	1.943(5)	1813[h]	71
[Ru(OEP)(NO)(ONO)]	2.060(5)	1.758(7)	174.0(8)	1.177(9)		1.984(6)	1835[h]	69
[Ru(TPP)(NO)(ONO)][j]	2.047(5)	1.72(2)	180.0[f]	1.12(2)	0.0[g]	1.90(2)	1854[h]	69
[Ru(TPP)(NO)(ONO)][j]	2.050(5)	1.72(2)	180.0[f]	1.19(3)		2.00(2)	1852[g]	63
[Ru(TTP)(NO)(ONO)]	2.053(6)	1.752(6)	173.3(6)	1.152(9)	0.13	1.998(6)	1835[h]	71
[Ru(OEP)(NO)(O=C(Me)$NHCH_2C(Me)_2SH$)]$^{+}$	2.050(8)	1.708(6)	177.8(5)	1.141(7)	0.10	2.049(4)	1856[h]	68
[Ru(TTP)(NO)(NSO)]	2.055(4)	1.737(5)	170.2(5)	1.160(6)		2.022(5)	1829[h]	67
[Ru(OEP)(NO)(S-NACysMe)]	2.053	1.790(5)	174.8(6)	1.123(8)		2.362(2)	1791[h]	53, 66
[Ru(OEP)(NO)($SC(Me)_2CH_2NHC(O)Me$)]	2.060(2)	1.769(3)	172.8(3)	1.114(4)	0.07	2.390(1)	1789[h]	68
[Ru(TTP)(NO)(*p*-C_6H_4F)]	2.05(2)	1.807	152	1.159		2.095(6)	1773[h]	72
[Ru(OEP)(NO)(*p*-C_6H_4F)]	2.059(7)	1.807(3)	154.9(3)	1.146(4)	0.12	2.111(3)	1759[h]	56
[Ru(OEP)(NO)($NOsO_3$)]	2.07(3)	1.83(2)	153(1)	1.26(2)		2.03(1)	1856[k]	73
[Ru(TTP)(NS)(Cl)]	2.049(2)	1.768(4)	169.1(3)	1.489(5)[l]		2.022(5)		67

[a] Value in Å. [b] Value in deg. [c] Displacement of the metal atom out of the 24-atom porphyrin plane toward the nitrosyl group. [d] Value in cm^{-1}. [e] Disorder required by inversion symmetry. Axial ligand distances affected. [f] Absolute value of 180.0° required by symmetry. [g] Metal within the porphyrin plane by crystallographic symmetry. [h] KBr pellet. [i] More accurate metal−ligand bond distance prevented by ligand disorder. [j] Severe axial ligand disorder, required by crystallographic symmetry. [k] Nujol mull. [l] N−S bond distance.

contain σ-bonded aryls and alkyls. The structure determination shows that the presence of a strongly σ-bonding ligand affects the electronic and geometric structure leading to the nonlinear FeNO group and to coordinated NO displaying a structural trans effect. Preliminary DFT calculations are consistent with the observed geometry being the lowest energy state of the molecule.

Complexes possessing both nitrite and nitric oxide as the axial ligands, with a variety of porphyrin ligands, have been prepared and structurally characterized with iron(III).[55] Although there has been some controversy concerning synthetic procedures for their synthesis,[60−62] these species are clearly distinct from the iron(II) species already discussed. As in the iron(II) systems, the nitrite anion binds through the nitrogen atom to form nitro complexes. The near equivalence in size and shape of both axial ligands leads to problems in distinguishing between them. This has severe, deleterious effects on the accurate determination of axial bond lengths and angles. In some disordered cases such as TPP and, surprisingly, OEP, it was impossible to distinguish between the two ligands. Use of picket fence porphyrin with its two inequivalent porphyrin faces allowed the two axial ligands to be distinguished. It was found that either nitric oxide or the nitrite ligand coordinates within the pocket of the porphyrin depending upon the synthetic method used.[55] The Fe−N(NO) bond lengths are equivalent to other iron(III) systems, and the Fe−N(NO_2) bond lengths are also comparable to other iron(III) systems, confirming the absence of a substantial trans effect in these systems. The one completely ordered nitro/nitrosyl iron(III) system has an Fe−N−O angle of 169.3°. This leads to the question of whether this small deviation from linearity is a real and intrinsic property of the mixed ligand system. (The required 2-fold axis of symmetry for another derivative and a slightly larger thermal parameter of the nitrite oxygen atom would likely obscure any such distortion.) It is our opinion that this small deviation is indeed real and intrinsic.

A comparison of the Fe−N(NO) bond lengths for all the iron(III) derivatives reveals one major disparity: the structure of [Fe(TPP)(NO)(HO-*i*-C_5H_{11})]-ClO_4.[53] This species has an anomalously large reported Fe−N(NO) bond distance of 1.776(5) Å, nearly 0.1 Å longer than all other iron(III) systems, and a very short N−O(NO) bond of 0.925(6) Å. As we described in the section on coordination geometry of the nitrosyl ligand, such an anomalously short N−O bond almost certainly is the result of either a disorder problem or the presence of an impurity in the crystal. We note that the observed ν(NO) does not suggest the presence of an unusual Fe−NO interaction.

2. Ruthenium and Osmium Derivatives

We now shift our focus to the nitrosyl derivatives of the remaining two metals of group 8: ruthenium and osmium. Unlike the iron systems, the nitrosyl complexes of either ruthenium or osmium in the 2+ oxidation state are not observed. That is, {MNO}^{7} porphyrin systems are known only for iron. Exactly which electronic feature leads to this uniqueness for iron nitrosyls is not clear and warrants further investigation. Another additional difference is that all ruthenium or osmium nitrosyl derivatives that have been isolated and structurally characterized are exclusively six-coordinate; no five-coordinate complexes are reported. With two notable exceptions that are discussed later, the ruthenium systems all contain RuNO moieties that can be described as nominally linear.[53,56,63−73] Bond lengths and angles for these ruthenium systems can be found in Table 5. Comparisons of structural details for species with identical axial ligands, e.g., the hydroxo and nitrito complexes, suggest that the overall level of precision of the ruthenium structures is somewhat lower than that of the iron derivatives. The value of the Ru−N(NO) bond distance is probably in the range of 1.74−1.77 Å; the reality of small deviations of the RuNO group from linearity is unclear. The small displacement of ruthenium toward nitric oxide is similar to that seen in the {FeNO}^{6} species.

Table 6. Summary of Coordination Group Geometry for (Nitrosyl)Osmium Metalloporphyrin Derivatives

complex	Os−N_p[a]	Os−N_{NO}[a]	∠OsNO[b]	N−O[a]	Δ[a,c]	Os−L[a]	ν(NO)[d]	ref
[Os(TTP)(NO)(S-*i*-C_6H_{11})][e]	2.058(8)	2.041(7)	172.0(9)	1.086(10)	0.03	2.209(3)	1760[f]	53
{[Os(OEP)(NO)]$_2$O}	2.066(5)	1.778(11)	180.0[g]	1.143(13)	0.23	2.0945(5)	1770[f]	75
[Os(OEP)(NO)(O-*n*-Bu)][i]	2.056(8)	1.833(8)	172.8(8)	1.173(11)		1.877(7)	1743[f]/1757[h]	76
[Os(OEP)(NO)(O_2PF_2)]	2.061(6)	1.711(6)	174.3(6)	1.179(8)	0.16	2.046(5)	1808[f]/1820[h]	76
[Os(OEP)(NO)(OEt)][i]	2.074(6)	1.81(2)	156.1(17)	1.33(2)	0.0	1.89(2)	1756[f]/1759[h]	77
[Os(OEP)(NO)(OH_2)]$^+$	2.061(6)	1.726(6)	176.6(6)	1.153(9)	0.18	2.071(5)		77
[Os(OEP)(NO)(HOEt)]$^+$	2.037(4)	1.720(4)	178.5(3)	1.167(5)	0.21	2.062(3)	1814[f]/1828[h]	77
[Os(OEP)(NO)(HO(CH_2)$_5$$CH_3$)]$^+$	2.057(6)	1.740(6)	174.4(6)	1.159(9)	0.22	2.097(5)	1754[f]/1757[h]	77
[Os(OEP)(NO)(HO(CH_2)$_5$$CH_3$)]$^+$ [j]	2.051(6)	1.728(7)	176.8(7)	1.174(9)	0.22	2.073(5)		77
[Os(OEP)(NO)(HOR)]$^+$ [k]	2.057(3)	1.709(4)	176.3(3)	1.186(5)	0.19	2.075(3)		77

[a] Value in Å. [b] Value in deg. [c] Displacement of the metal atom out of the 24-atom porphyrin plane toward the nitrosyl group. [d] Value in cm^{-1}. [e] Axial ligand disorder. [f] KBr pellet. [g] Exact value required by crystallographic symmetry. [h] CH_2Cl_2 solution. [i] Axial ligand disorder required by inversion center. [j] Second molecule. [k] Crystal contains a mixture of two alcohols, EtOH and ^{i}PrOH.

An examination of Table 5 reveals that most of the characterized derivatives have an oxygen donor trans to the nitric oxide; in particular, there are no derivatives with neutral nitrogen donors. That the ruthenium derivatives coordinate to nitrite ion via an oxygen atom rather than the nitrogen atom as in the iron derivatives is surprising given the iron(II) and -(III) results already described. One possible explanation might be that the relative propensities of the iron(III) and ruthenium(III) complexes to π bond to ligands in addition to NO are different.

The series of complexes with either nitrite or hydroxide as the sixth ligand allows a consideration of the effects of porphyrin macrocycle variation upon the overall structure. The complexes structurally characterized are for three different porphyrin ligands: TPP,[63,69] TTP,[71] and OEP.[69] Within reasonable error limits, there is no effect of the porphyrin. In these derivatives, as has been noted earlier,[33,74] the porphyrin ligand, and not the small axial ligands, controls the solid-state packing of the molecules. Thus, both TPP derivatives are isomorphous; the two OEP derivatives also form an isomorphous series.

Two ruthenium systems reported by Richter-Addo and co-workers[53,66,68] have a thiolate ligand trans to NO. Both systems are conveniently prepared by a ligand replacement/oxidative addition in which a thionitrite (S-nitroso, RSNO) reacts with a ruthenium(II) carbonyl to yield a trans thiolate/nitrosyl ligand combination. One such thiolate ligand is an L-*N*-acetylcysteinate methyl ester. The possible reaction of such reagents in hemes has been suggested as biologically significant. Complexes of this sort can also be prepared by the direct replacement of a ligand trans to NO by a thiolate derivative. Structural features of these thiolate-ligated species do not appear to be unusual. The thiolate ligand can be displaced when protonated by a strong acid.

The two exceptions to linear RuNO geometry are the systems containing the *p*-fluorophenyl (*p*-C_6H_4F) group as the sixth ligand. This σ-bonded aryl ligand system has been characterized for two different porphyrins: TTP[56,72] and OEP.[56] Here, as in the iron(III) system, the Ru−N−O group does not display the expected linearity and instead is found to be ∼155° for both systems. The bending of the RuNO unit was not initially recognized as an intrinsic feature of the molecule and was originally interpreted to arise from steric and crystal packing effects. However, the fact that this behavior is observed for two different metals and two different porphyrin systems leads to the conclusion that the M−N−O bending arises from the influence of the sixth trans ligand.

Three derivatives listed in Table 5 have especially novel axial ligands. The nitrosyl thiazate derivative, [Ru(TTP)(NO)(NSO)], has two axial nitrogen donors.[67] The structural features appear to be similar to those of other ruthenium derivatives; the Ru−N−S angle is 140.8(3)°. This complex was prepared from the thionitrosyl derivative [Ru(TTP)(NS)(Cl)], whose structural parameters are listed in Table 5.[67] To our knowledge, this derivative is the only known example of metalloporphyrin containing a coordinated thionitrosyl. The third species is a binuclear species with a bridging nitride ligand that bridges to an osmium center.[73] The species is reported to have a bent nitrosyl group; however, the nitrosyl stretching frequency seems to be very high for such a structural feature.

In contrast to all other metal nitrosyl systems considered, the osmium nitrosyls show the widest variation in the geometrical parameters associated with the MNO unit. Much of this may be an effect of the very heavy osmium atom and the attendant difficulty in obtaining highly accurate structures. Like ruthenium, only complexes that can be classified as {MNO}^{6} species are observed, all of which contain the nominal osmium(III) ion. Bond lengths and angles for all these complexes are listed in Table 6.[53,75−77] With one exception, these compounds all contain a linear OsNO unit. The exception is the ethoxide complex [Os(OEP)(NO)(OEt)][77] for which an Os−N−O angle of 152° is reported. No explanation was originally provided for this unexpected geometry, and we are also unable to offer an explanation that is consistent with the structures of the other osmium and ruthenium derivatives.

The most interesting of the osmium nitrosyl species reported is the binuclear μ-oxo species {[Os(OEP)(NO)]$_2$O}·2HCl.[75] This consists of two [Os(OEP)(NO)] units linked by a single oxygen atom bridge as shown in Figure 17. The OsNO units are found to be linear, lying on a 4-fold axis of symmetry while the oxygen atom lies on a higher-symmetry special position. This gives a linear {O−N−Os−O−Os−N−O} group, while the porphyrin macrocycles are 1/4 unique. The porphyrins are slightly domed; the osmium is displaced from the mean porphyrin plane by almost 0.3 Å

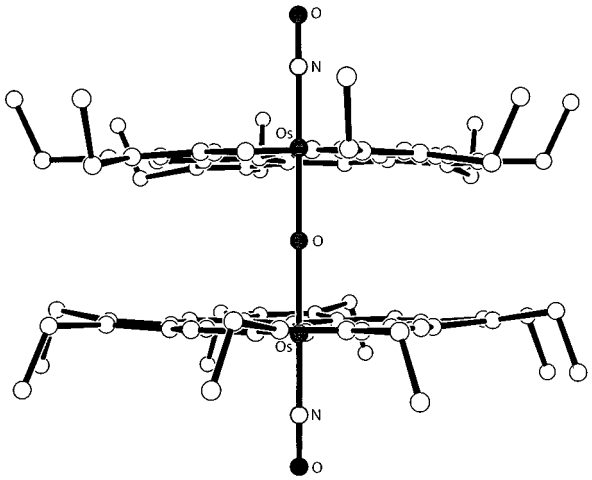

Figure 17. Molecular diagram of the osmium μ-oxo dimer, {[Os(OEP)(NO)]$_2$O}. The absolute linear nature of the O−N−Os−O−Os−N−O vector is imposed by crystallographic symmetry. Coordinates taken from ref 75.

toward the NO, and the ethyl groups all point away from the adjacent bridged macrocycle. The two porphyrins are also rotated slightly from each other, giving a twist angle of ~22.5°.

III. Nitrite and Nitrate Derivatives

A. Nitrite Derivatives

The interaction of nitrite ion with heme proteins occurs in denitrification and terminal electron acceptor processes. The nitrite is presumed to bind at a heme site, which is considered the catalytic site. A number of metalloporphyrin complexes that contain coordinated nitrite ion have been characterized. Several examples of (nitro)nitrosyl complexes have already been mentioned in previous sections. We now examine the nitrite ligand in more depth, considering both those nitrite systems that contain a nitrosyl ligand and those that do not. For some systems, the importance of π back-bonding to nitrite is evident, while in others, it may be a secondary issue. As has already been noted, the effects of having two competing π acceptor ligands in the same molecule can be analyzed in structural terms. In the coordination chemistry of nitrite coordinated to metalloporphyrins, the most important of the metalloporphyrin derivatives are those of iron.

Early attempts to isolate an iron(III) porphyrinate system with a coordinated nitrite ligand were unsuccessful due to a facile oxygen atom transfer reaction from coordinated nitrite to yield the five-coordinate iron(II) nitrosyl complex.[78] The instability of the iron(III) nitrite system appears to result from the extreme thermodynamic stability of the iron(II) nitrosyl. Thus, an attempt to carry out simple ligand exchange processes (as illustrated below) yields the nitrosyl and nitrato complexes. The reactive species is almost certainly the nitrite complex [Fe(Por)(NO$_2$)].

$$2[\mathrm{Fe(Por)(X)}] + 2\mathrm{NO_2^-} \rightarrow [\mathrm{Fe(Por)(NO)}] + [\mathrm{Fe(Por)(NO_3)}] + 2\mathrm{X^-}$$

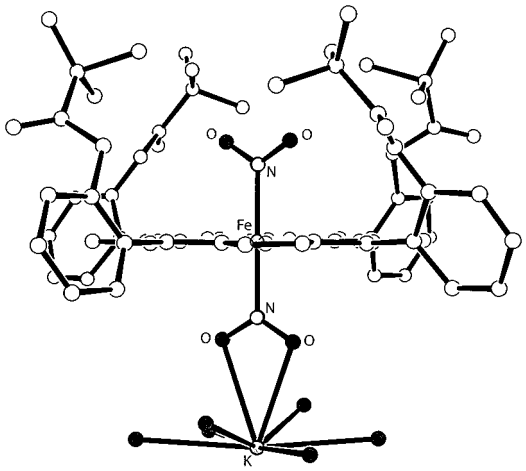

Figure 18. Molecular diagram of the bis-nitrite species [K(18-C-6)(H$_2$O)][Fe(TpivPP)(NO$_2$)$_2$]. Carbon atoms of the 18-crown-6 and the water molecule are not represented. Coordinates are taken from ref 79.

One solution to the instability problem was to use a porphyrin with a protected ligand binding site. The use of picket fence porphyrin resulted in the isolation and structural characterization of the bis(nitrite) complex [K(18-C-6)(H$_2$O)][Fe(TpivPP)(NO$_2$)$_2$];[79] this species is also the synthetic entry into other nitrite complexes of iron(III). The nitrite bound within the pocket of the porphyrin is afforded a measure of protection by the picket arms. The nitrite ion bound to iron on the open face is also protected against oxygen atom transfer reactions by the formation of a tight ion pair with the encapsulated potassium counterion. A side view of this structure is shown in Figure 18. Both nitrites are found to be η^1-N coordinated, and although inherent disorder in the structure prevents absolute determination of the relative orientations of the two nitrite planes, it is thought that they have relative parallel orientations. Such a relative orientation of the two axial ligands is most consistent with the observed rhombic EPR spectrum. The in-pocket nitrite group has the longer of the two Fe−N(NO$_2$) distances and is just statistically significant (4σ). This bond length is generally found to decrease upon the replacement of the out-of-pocket nitrite by a neutral sixth ligand.

Mixed ligand (nitrite)iron(III) complexes have been characterized for both N-donor[80] and S-donor[29] ligands, and data for these and other nitrite complexes are given in Table 7. For the pyridine and imidazole adducts,[80] the nitrite ligand is found to lie approximately between a pair of Fe−N$_p$ bonds, while the nitrogen ligand plane is oriented in a relative perpendicular orientation, lying between the adjacent pair of Fe−N$_p$ bonds. Additionally, the Fe−N(L) ligand distance is slightly longer than those of the bis-ligated pyridine and imidazole species. The structure of [Fe(TpivPP)(NO$_2$)(HIm)] is shown in Figure 19. The precise value of the dihedral angle between the nitrite plane and the closest Fe−N$_p$ vector is given as ϕ in Table 7. This angle nearly bisects an adjacent pair of Fe−N$_p$ vectors in all cases. While such an angle is sensible on steric grounds, an analysis of the fitting of the principal axis systems of the $\tilde{g}$ and $\tilde{A}$ tensors obtained from Mössbauer

Table 7. Summary of Coordination Group Geometry for Nitrite-Coordinated Metalloporphyrin Derivatives

A. Nitro derivatives

complex	M−N_p[a]	M−N(NO_2)[a]	N−O(av)[a]	ϕ[b,c]	Δ[a,d]	M−L[a]	ν(NO_2)[e]	ref
Iron(III) derivatives								
[Fe(TpivPP)(NO_2)$_2$]$^-$	1.992(1)	2.001(6)[f] 1.970(5)[h]	1.233[f] 1.239[h]	37[f] 34[h]	0.01		1315/1351[g]	79
[Fe(TpivPP)(NO_2)(Py)]	1.983(3)	1.960(5)	1.233(4)	37	−0.04	2.093(5)	1341/1390[g]	80
[Fe(TpivPP)(NO_2)(HIm)]	1.970(4)	1.949(10)	1.191(8)	37	−0.02	2.037(6)	1310/1341[g]	80
[Fe(TpivPP)(NO_2)(SC_6HF_4)]$^-$	1.980(7)	1.990(7)	1.223(7)	32	−0.05	2.277(2)	1352[g]	29
[Fe(TpivPP)(NO)(NO_2)]	2.000(5)	2.002(2)	1.270(5)		−0.15	1.668(2)		55
[Fe(TpivPP)(NO)(NO_2)]	1.996(4)	1.998(2)	1.223(4)	44.1	−0.09	1.671(2)		55
Iron(II) derivatives								
[Fe(TpivPP)(NO_2)]$^-$	1.970(4)	1.849(6)	1.243(7)	40.4	0.18			48, 82
[Fe(TpivPP)(NO_2)(Py)]$^-$	1.990(15)	1.951(5)	1.257(5)	42	−0.04	2.032(5)	1289/1354[g]	82
[Fe(TpivPP)(NO_2)(PMS)]$^-$	1.990(6)	1.937(3)	1.242(4)	44	−0.01	2.380(2)	1295/1349	82
[Fe(TpivPP)(NO)(NO_2)]$^-$ [i]	1.988(6)	2.086(8)	1.245(8)	44.1	−0.10	1.792(8)	1310/1380[g]	49
[Fe(TpivPP)(NO)(NO_2)]$^-$ [j]	1.986(6)	2.060(7)	1.243(8)	44	−0.09	1.840(6)	1305/1346[k]	49
Cobalt(III) derivatives								
[Co(TPP)(NO_2)(3,5-Lut)]	1.954(4)	1.948(4)	1.153(4)	1.6		2.036(4)		84
[Co(TPP)(NO_2)(Pip)]	1.953(9)	1.897(11)				2.044(10)		85
[Co(TpivPP)(NO_2)(I-MeIm)]	1.964(4)	1.898(4)	1.223(3)	39.4	−0.04	1.995(4)		83
[Co(TpivPP)(NO_2)(1,2-MeIm)]	1.983(4)	1.917(4)	1.227(3)	34.9	−0.08	2.091(4)		83
[Co(Tpp)(NO_2)(Py)][i,l]	1.969(4)	1.920(4)	1.200			2.032(4)	814/1309/1425[g]	86
[Co(TPP)(NO_2)(Py)][j,l]			1.219				814/1309/1425[g]	86
[Co(TPP)(NO_2)(Cl_2Py)]	1.954(3)	1.912(3)	1.217			2.044(3)	817/1309/1424	86

B. Nitrito derivatives

complex	M−N_p[a]	M−O1(NO_2)[a]	O1−N[a]	N−O2[a]	∠O1−N−O2[c]	ν(NO_2)[e]	ref
Ruthenium(III) derivatives							
[Ru(TPP)(NO)(ONO)]	2.050(5)	2.00(2)	0.94(5)	1.33(4)	109(5)	932/1520[g]	63
[Ru(TPP)(NO)(ONO)]	2.047(5)	1.90(2)	1.16(2)	1.23(2)	108.0(30)	930/1522[g]	69
[Ru(OEP)(NO)(ONO)]	2.060(7)	1.984(6)	1.214	1.188(9)	117.3(9)	963/1497[g]	69
[Ru(TTP)(NO)(ONO)]	2.053(6)	1.988(6)	1.15(2)	1.13(3)	110.9(20)	927/1511[g]	71
Manganese(III) derivative							
[Mn(TPP)(ONO)]	2.012(5)	2.059(4)	1.301(7)	1.202(8)	114.8(5)	682/1029/1444[g]	87

[a] Value in Å. [b] Dihedral angle between nitrite plane and closest M−N_p vector. [c] Value in deg. [d] Displacement of the metal atom out of the 24-atom porphyrin plane toward the nitrite group. Negative numbers indicate displacement away from nitrite. [e] Value in cm^{-1}. [f] Nitrite located in pocket. [g] KBr pellet. [h] Nitrite located on open-face. [i] ⊥ form. [j] || form. [k] Nujol mull. [l] Single crystal, nitrite disordered, 50% parallel to pyridine plane, 50% perpendicular to pyridine plane.

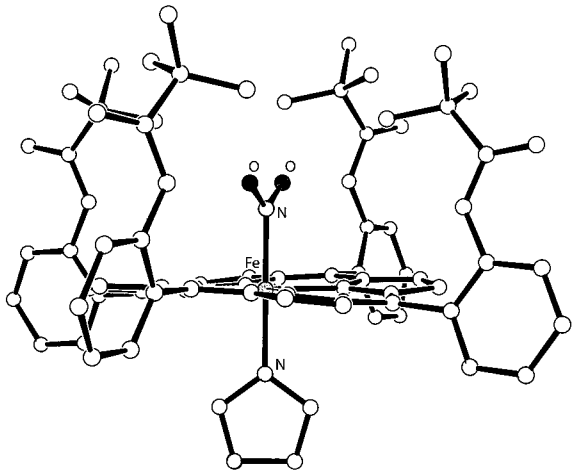

Figure 19. Molecular diagram of the mixed ligand nitrite complex [Fe(TpivPP)(NO_2)(HIm)]. Note the relative orientation of the two axial ligand planes. Drawn from coordinates reported in ref 80.

spectra on [Fe(TpivPP)(NO_2)(HIm)] and [Fe(TpivPP)(NO_2)(Py)] in an 8 T applied magnetic field also suggests that the orientation of the nitrite plane defines the orientation of the dπ (d_{xz} and d_{yz}) orbitals.[80] The orientation suggested by the Mössbauer analysis has the plane of the two dπ (d_{xz} and d_{yz}) orbitals parallel and perpendicular to the nitrite plane, consistent with maximizing the π acceptor capabilities of the N-bound nitrite. This analysis is also supported by the large value of the rhombicity calculated from an analysis of the EPR spectra of both the bis(nitrite) complex and the mixed nitrite/pyridine and imidazole complexes.[80] A single-crystal EPR study has confirmed the assigned coordinate system.[81] A similar analysis for the mixed ligand complex [Fe(TpivPP)(NO_2)(S−C_6HF_4)],[29] which contains both the strong π acceptor ligand nitrite and a possible π donor in the trans thiolate, shows that the nitrite ion dominates the binding mode and ligand orientations. The strong π-accepting character of nitrite led to attempted synthesis of a five-coordinate iron(III) species, which would be expected to be low spin. All attempts have been unsuccessful, apparently due to the oxygen-atom transfer reactivity and the formation of the nitrosyl.

However, it is possible to successfully isolate five-coordinate iron(II) nitrite complexes, and the anionic, five-coordinate, low-spin [Fe(TpivPP)(NO_2)]$^-$ complex has been reported.[48,82] The η^1-N bonded nitrite ligand is coordinated within the porphyrin pocket with an

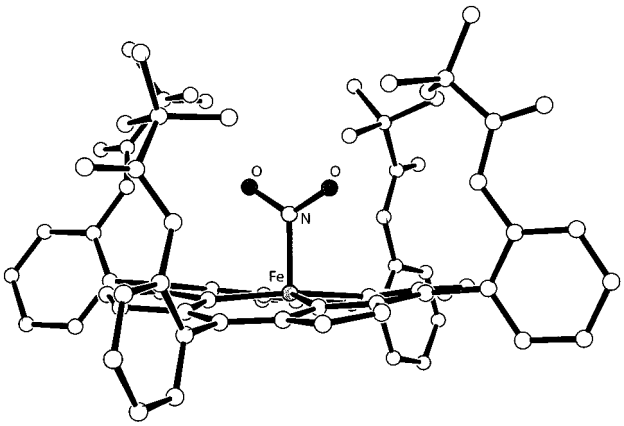

Figure 20. Molecular diagram of five-coordinate [Fe(TpivPP)(NO_2)]$^-$. Drawn from coordinates reported in ref 82.

adventitious water molecule located at the mouth of the pocket that is weakly hydrogen bonded to the two nitrite oxygen atoms. The Fe−N(NO_2) bond length of 1.849(6) Å is substantially shorter than expected, especially compared to the iron(III) systems already discussed. The iron atom is displaced by only 0.18 Å from the porphyrin plane, and the equatorial Fe−N_p bond distance is 1.970(4) Å, consistent with a low-spin state. Again, the nitrite plane is located about midway between a pair of Fe−N_p bonds with a dihedral angle of 40.4°, very similar to the iron(III) systems. Figure 20 displays the stereochemistry of the five-coordinate species.

The low-spin nature of this mononitrite species and the fact that the nitrite ligand is located between a pair of Fe−N_p bonds serve to emphasize the strong π acceptor nature of the nitrite ligand in this iron(II) species. A final feature strongly consistent with strong π acceptor character of the nitrite ligand is the anomalously large value of the quadrupole doublet in the zero-field Mössbauer. The large value of 2.28 mm/s for the quadrupole splitting is strongly suggestive of the stabilization of one of the two dπ orbitals by Fe−NO_2 π back-bonding. The Mössbauer spectrum in an applied magnetic field confirms the low-spin (diamagnetic) ground state.[48,82]

Six-coordinate iron(II) derivatives can be prepared by straightforward addition of the sixth ligand to an anaerobic solution of the mononitrite species.[82] Examples have been prepared for both neutral N-donor (pyridine) and S-donor (pentamethylene sulfide) ligands. As was observed for the iron(III) mixed ligand systems, the iron is located slightly out of plane toward the sixth ligand, while the nitrite plane is oriented midway between a pair of Fe−N_p bonds. For the pyridine complex, a relative perpendicular orientation of the two axial ligands is observed and a slight ruffling of the porphyrin core is also evident. The Fe−N(NO_2) bonds are found to be longer for the six-coordinate complexes compared to the five-coordinate species by ∼0.1 Å. This increase in the Fe−N(NO_2) distance seems unlikely to be caused solely by steric interactions, since similar elongations in Fe−N(NO) distances are not observed between the six-coordinate and five-coordinate iron nitrosyl complexes in either oxidation state. This observation led Nasri et al.[82] to suggest that in the five-coordinate complex, the nitrite acts as a very strong π acceptor, but this capability is diminished upon coordination of a sixth ligand even when the sixth ligand is not a strong π bonder. This notion led to the characterization of the nitrite in the iron(II) systems as a "highly variable" π-bonding ligand.

Both iron(II) and -(III) complexes of the general formula [Fe(por)(NO)(NO_2)]$^{-/0}$ have also been prepared.[49,55] For the iron(II) systems,[49] picket fence porphyrin derivatives were studied and two distinct crystalline forms were found. The two differ in the relative orientations of the axial ligands with the ligands being coordinated either in relative perpendicular or parallel orientations to each other. In both cases, the nitrite is coordinated in the porphyrin pocket and midway between a pair of Fe−N_p bonds. The angles between the nitrite and nitrosyl planes are found to be 85.4 and 20.9°, respectively. The Fe−N(NO_2) bond lengths are found to be longer (∼0.13 Å) than other iron(II) species, possibly reflecting the strong trans effect exhibited by the nitrosyl ligand. The corresponding Fe−N(NO) bond length is also longer than in other {FeNO}^{7}systems, possibly indicating a decreased π interaction for the NO ligand as well.

For the iron(III) systems, difficulties are encountered in dealing with two axial ligands that are nearly equivalent and difficult to differentiate. The picket fence porphyrin allows not only a protected ligand binding site but also the two faces of the porphyrin to be distinguished. The nitrite is found to be located within the pocket of the porphyrin, albeit in a predominant location only. There is a small degree of axial ligand in/out disorder observed. Again the nitrite is located between a pair of Fe−N_p bonds, although the linear nature of the nitrosyl ligand in this {FeNO}^{6} system renders the relative ligand orientations moot. There is a small increase in both axial bond distances compared to complexes with a single nitrosyl or nitrite ligand, but the increases are substantially smaller than those found for the iron(II) systems.

A similar η^1-N coordination mode of the nitrite ligand is observed for all the cobalt complexes that have been structurally characterized. Two complexes, [Co(TpivPP)(NO_2)(1-MeIm)] and [Co(TpivPP)(NO_2)(1,2-MeIm)], have been prepared[83] using the protected ligand binding site principle already described for the iron systems, and like the iron systems, the nitrite ion is found to coordinate within the pocket. However, due to the reduced reactivity of the cobalt(III) system, it is possible to successfully isolate nitroporphyrinate systems using open-face porphyrins, although the five-coordinate mono(nitrite) system remains elusive. For the tetraphenylporphyrin system, [Co(TPP)(NO_2)(3,5-Lut)],[84] [Co(TPP)(NO_2)(Pip)],[85] [Co(TPP)(NO_2)(Py)],[86] and [Co(TPP)(NO_2)(Cl_2Py)][86] have been successfully characterized. All the cobalt complexes exhibit a N-bound nitrite group trans to a neutral N-donor ligand. [Co(TPP)(NO_2)(3,5-Lut)] possesses a highly ruffled porphyrin core with larger than usual displacement of the methine carbons from the mean porphyrin plane. These displacements (0.56

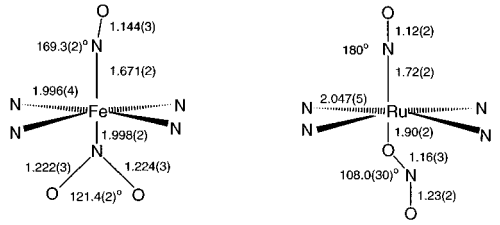

Figure 21. Comparison of coordination geometry for the iron(III) and ruthenium(III) (nitro)nitrosyl complexes. Bonding parameters for [Fe(TpivPP)(NO)(NO_2)] and [Ru(TPP)NO(NO_2)] are taken from refs 55 and 69, respectively.

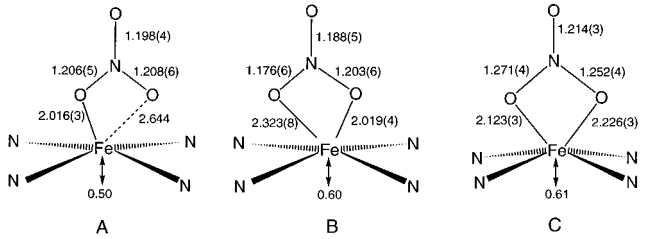

Figure 22. Schematic representation of the three coordination modes of the nitrate ligand. Bonding parameters for the (A) monodentate, (B) asymmetric bidentate, and (C) symmetric bidentate modes are taken from the structures [Fe(OEP)(NO_3)],[88] [Fe(TPP)(NO_3)],[90] and [Fe(TpivP)(NO_3)],[91] respectively.

and −0.64 Å) are substantially larger than those observed for other ruffled systems, especially those without peripherally crowded substituents. The nitrite ligand is nearly coincident with one pair of Co−N_p bonds giving a small dihedral angle (ϕ) of 1.6°. This is especially unusual compared to both the iron and the cobalt picket fence systems where the dihedral angles were consistently found to ∼40−45°. The axial bond to the lutidine ligand is longer than expected, a fact partially attributed to steric interactions between the ortho-hydrogens of the lutidine and the porphyrinato nitrogen atoms. The lutidine is oriented close to the Co−C_m vector with an effective dihedral angle of 36.4°, which effectively minimizes the steric interactions between the ligand and the porphyrin. An angle of 52° is thus observed between the two axial ligand planes. Similar ruffling of the porphyrin core is observed for the [Co(TPP)(NO_2)(Pip)] system, although in this case, the sixth ligand, piperidine, is not planar and determination of ligand orientation is more complicated. Core ruffling is reduced dramatically for both the picket fence and the pyridine/dichloropyridine systems. Bonding parameters for all of the cobalt(III) complexes are given in Table 7. The unusually short Co−N(1-MeIm) bond observed for the [Co(TpivPP)(NO_2)(1-MeIm)] system is rationalized on the basis of the smaller steric bulk of the ligand compared to that of the larger lutidine and piperidine systems. Like the iron nitrite systems, the cobalt is invariably displaced from the porphyrin plane in the direction of the non-nitrite ligand. This is in contrast to the nitrosyl systems where displacement is always in the direction of the nitrosyl.

As mentioned previously, the nitrite ligand is an ambidentate species and can vary in the coordination mode to a metal center. A second possible binding mode is the η^1-O or nitrito, a mode observed for both ruthenium and manganese porphyrinate systems. Three nitrito(nitrosyl) complexes have been reported for three different ruthenium porphyrinates: OEP,[69] TPP,[63,69] and TTP.[71] The nitrosyl aspect of these complexes has already been discussed in the previous section, while apart from the unexpected coordination mode of the nitrite group, these complexes are unremarkable in their bond lengths and angles. A comparison of the bonding parameters for both ruthenium and iron (nitro)nitrosyl complexes is shown in Figure 21. Nitrito coordination is also observed for the manganese system [Mn(TPP)(NO_2)],[87] with the nitrite ligand in this five-coordinate complex being coordinated in a monodentate fashion via one of the oxygen atoms. There is a clear difference in the two N−O bond lengths with the unligated N−O bond being shorter and indicative of more double-bond character.

B. Nitrate Derivatives

In all metalloporphyrin derivatives, nitrate coordination is exclusively through the oxygen atom(s). Bonding parameters for all reported metalloporphyrin nitrate complexes[87−93] are given in Table 8. In a series of iron(III) derivatives, an interesting aspect of the nitrate ligand coordination is that the denticity of nitrate displays wide variation for different high-spin complexes of the general formula [Fe(Por)(NO_3)]. In each of these, nitrate is the sole axial ligand. As illustrated schematically in Figure 22, the coordination mode of the ligand varies from a monodentate fashion to a nearly symmetrical bidentate mode.

The first complex, [Fe(OEP)(ONO_2)],[88] has a monodentate nitrate group. The nitrate is coordinated in a very asymmetric fashion with an Fe−O(ONO_2) bond length of 2.016(3) Å, an Fe−O−N angle of 115.8 (3)°, rather unequal N_p−Fe−O angles, and the nitrate plane between a pair of Fe−N_p bonds with a dihedral angle (ϕ) of 31°. A second crystalline derivative of [Fe(OEP)(ONO_2)] is more symmetric with a shorter Fe−O distance.[89] The TPP system, [Fe(TPP)(O_2NO)],[90] possesses a bidentate nitrate ligand with Fe−O(NO_3) bond lengths of 2.323(8) and 2.019(4) Å. The nitrate plane lies exactly between a pair of Fe−N_p bonds with a dihedral angle of 45°. As with the OEP systems, the iron is substantially displaced from the mean porphyrin plane with an out-of-plane displacement of 0.60 Å for the TPP system, compared to 0.50 Å for the OEP complex. The final iron system that has been characterized is the picket fence complex [Fe(TpivPP)(O_2NO)],[91] illustrated in Figure 23. This complex was obtained from attempts to isolate a stable mono(nitro)iron porphyrinate and has a nitrate ligand coordinated in a nearly symmetrical fashion. However, unlike the TPP system, the nitrate ligand plane lies almost coincident with an opposing pair of Fe−N_p bonds with a dihedral angle of 10°. The two opposite pairs of Fe−N_p bonds can be described as long (average 2.083 Å) and short (average 2.060 Å). The nitrate group plane is found to almost eclipse the longer pair of bonds. The two Fe−O(NO_3) bond lengths are 2.123(3) and 2.226(3) Å, and the iron is significantly displaced from the mean porphyrin plane.

Table 8. Summary of Coordination Group Geometry for Nitrate-Coordinated Metalloporphyrin Derivatives

complex	M−N_p[a]	M−O(NO_3)[a]	N−O[a]	Δ[a,b]	φ[c,d]	ν(NO_3)[e]	ref
[Fe(OEP)(ONO_2)][f]	2.056(1)	2.016	1.206(5) 1.198(4) 1.208(6)	0.50	31	1515[g]	88
[Fe(OEP)(ONO_2)][h]	2.047(6)	1.966(2)	1.301(3) 1.212(3) 1.199(3)	0.45	41		89
[Fe(TPP)(O_2NO)]	2.073(12)	2.323(8) 2.019(4)	1.176(6) 1.203(6) 1.188(5)	0.60	45	1275/1544[g]	90
[Fe(TpivP)(O_2NO)]	2.071	2.123(3) 2.226(3)	1.271(4) 1.252(4) 1.214(3)	0.61	10		91
[Mn(TPP)(ONO_2)]	2.007	2.101(3) 3.151(4)	1.298(5) 1.226(5) 1.226(5)	0.20		1286/1385/1474[i]	87
[MoO(TPP)(ONO_2)]	2.089	2.243(2)		−0.39		1280/1386/1476[i]	92
[Co(OEP′)(O_2NO)][j]	1.91	2.03(1) 2.07(1)	1.28(1) 1.26(1) 1.28(1)				93

[a] Value in Å. [b] Displacement of the metal atom out of the 24-atom porphyrin plane toward the nitrate group. Negative numbers indicate displacement away from nitrate. [c] Value in deg. [d] Dihedral angle between the nitrate plane and the closest M−N_p plane. [e] Value in cm^{-1}. [f] Triclinic form. [g] Nujol mull. [h] Monoclinic form. [i] KBr pellet. [j] This complex contains a modified octaethylporphyrin as described in the main text.

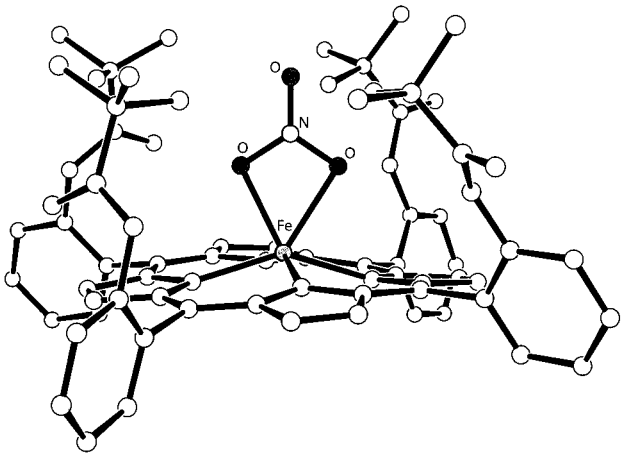

Figure 23. Molecular diagram of the picket fence nitrate complex [Fe(TpivPP)(NO_3)]. The side view emphasizes the highly symmetric coordination mode of the nitrate ligand. Drawn from coordinates reported in ref 91.

The variation in the interaction of nitrate with iron(III) from monodentate to (almost) symmetric bidentate changes the coordination number of iron from five to six and the symmetry of the iron environment from quasi-C_{4v} to quasi-C_{2v}. Such changes in the coordination geometry might be expected to significantly affect the electronic structure of iron. This question is currently being explored.[94]

One six-coordinate mixed nitrate/aquo iron(III) complex is also known.[95] The nitrate is monodentate with an Fe−O(ONO_2) bond distance of 2.02 Å. The trans water has a coordinated Fe−O(OH_2) bond distance of 2.18 Å. A five-coordinate, high-spin iron(II) complex is also known; the iron(II) atom is coordinated through a single oxygen atom.[96]

A few other other metal derivatives with a coordinated nitrate ligand are also known: those of manganese, molybdenum, and cobalt. The manganese(III) complex [Mn(TPP)(NO_3)],[87] unlike the analogous iron derivative, has a monodentate nitrate group coordinated in a very symmetric fashion. In fact, the Mn−O(ONO_2) vector is found to lie very close to the normal to the porphyrin plane, resulting in a large distance between the manganese center and the next closest oxygen of the nitrate group (3.151(4) Å). The molybdenum(V) species [MoO(TPP)(NO_3)][92] also has a monodentate nitrate group, although this six-coordinate complex has a metal atom displaced out of the porphyrin plane away from the nitrate. This may help in explaining the unusually long Mo−O(ONO_2) bond observed (2.24 Å). Interestingly, the Mo−O(ONO_2) vector is once again very close to the porphyrin normal and in an almost linear (176.5°) OMoO(ONO_2) unit, similar to other six coordinate molybdenum(V) porphyrin complexes and again resulting in a very asymmetrically coordinated nitrate group.

Interestingly enough, a cobalt nitrate complex with a modified octaethylporphyrin has also been characterized.[93] The porphyrin is modified by addition of two −(CH)CO_2Et units between a pair of adjacent pyrrolic nitrogens. This results in an increase of the distance between the cobalt and these nitrogens to ∼2.7 Å, ruling out the existence of a cobalt−nitrogen bond for these nitrogens. Instead, the carbon atom directly bonded to the nitrogen coordinates to the cobalt. The nitrate ligand in this complex is found to be coordinated in a very symmetrical bidentate fashion. In fact, the two M−O(NO_3) bond lengths are more similar than any of the other bidentate coordinated nitrate complexes.

IV. Related Protein Structures

We will cover only those protein crystal structures that have an NO_x ligand coordinated to the heme site of the enzyme. Further structural information for the proteins in the absence of these ligands is mentioned only in passing and only for comparison purposes. With three exceptions, the NO_x−heme systems are exclusively nitrosyl complexes. Although the interaction of NO with oxymyoglobin or oxyhemoglobin is a

Table 9. Protein NO Table

complex	resolution[a]	Fe−N_{NO}[a]	∠FeNO[b]	N−O[a]	Fe−L[a]	ref
		Iron(II) five-coordinate hemes				
(α-Hb)NO	2.8	1.74	145	1.1		100
(α-T-Hb_A)NO	2.2	1.74	150	1.13		101
(cyt *c*′)NO (**1**)[c]	1.35	2.0	124			109
(cyt *c*′)NO (**2**)[d]	1.35	2.0	132			109
(*e*NOS)NO(−4HB)[e,f]	2.00	1.80	160	1.14		110
(*e*NOS)NO(+4HB)[g,f]	2.30	1.80	160	1.15		110
(NP1)NO (**I**)[h]	2.3		125			116
(NP1)NO (**II**)[i]	2.3		135			116
(NP4)NO (**I**)[j]	1.4	2.0	110			117
(T243A-P450nor)NO	1.4					118
(T243N-P450nor)NO	1.4					118
(T243V-P450nor)NO	1.4					118
		Iron(II) six-coordinate hemes				
(β-Hb)NO[k]	2.8	1.74	145	1.1	NA[l]	100
(β-T-Hb_A)NO	2.2	1.74	155	1.12	2.30	101
(α-SNO-nitrosylHbA)NO	1.8	1.75	131	1.13	2.28	103
(β-SNO-nitrosylHbA)NO	1.8	1.74	123	1.11	2.28	103
(lupin-Lb^{II})NO	1.8	1.72	147		2.20	104
(Mb)NO	1.7	1.89	112	1.15	2.18	105
(L29F-Mb)NO			130		NA[l]	107
(SHP)NO	2.2	1.8	112		2.16[m]	108
(cd_1-NIR(*pa*))NO	2.65	1.8	135	1.15	1.99[m]	111
(cd_1-NIR(*tp*))NO	1.8	2.0	131		1.99[m]	112
(CCP)NO (**1**)[n]	1.85	1.82	135		2.04	113
(CCP)NO (**2**)[o]	1.85	1.82	125		2.04	113
(SiRHP)NO	1.80	1.76	125		2.65[p]	114
(soybean-Lb^{II})NO	MS-XAFS[q]	1.77	147	1.12[r]	1.98	119
		Iron(III) hemes				
(NP4)NO (**II**)[s]	1.4	1.5	177			117
(soybean-Lb^{III})NO	MS-XAFS[q]	1.68	173	1.12[r]	1.89	119

[a] Value in Å. [b] Value in deg. [c] Nitrosyl conformer **1**. [d] Nitrosyl conformer **2**. [e] Cofactor tetrahydrobiopterin absent. [f] Values reported are averaged for both subunits. [g] Cofactor tetrahydrobiopterin present. [h] Two molecules in asymmetric unit, molecule **I**. [i] Two molecules in asymmetric unit, molecule **II**. [j] Two orientations of NO observed, orientation **I**. [k] Differs from the α form by the orientation of NO with respect to the heme and the coordination number. [l] Not available. [m] Value not reported in original paper, obtained from Protein Data Bank. [n] Disordered oxygen, position 1. [o] Disordered oxygen, position 2. [p] Fe−S bond. [q] Structure determined by multiple scattering XAFS. [r] Bond length constrained to exactly 1.12 Å. [s] Two orientations of NO observed, orientation II.

facile reaction that yields nitrate and/or nitrate-coordinated derivatives,[97] and the interaction of (nitrosyl)hemoglobin with dioxygen also yields nitrate,[98] at the time of writing, no structural information for a protein containing a coordinated nitrate ligand has been reported. Nitrite is an important biological ligand/substrate, and three nitrite-bound protein structures have been reported.

Like the model complexes, the (nitrosyl)heme proteins can be classified on the basis of the nominal oxidation state of the metal. The reaction of heme proteins with NO frequently leads to reduction if the iron center is in the iron(III) state, perhaps explaining why the (nitrosyl)iron(II) heme proteins are more numerous. The systems can then be further divided into either five- or six-coordinate systems, although this is a more complicated classification than that in the small molecule systems. Frequently, the assignment of the coordination number of iron is not addressed in the published report. The ambiguous structural data in a few cases makes it difficult to clearly define the coordination number of the iron center. Bonding parameters for the (nitrosyl)heme systems, along with the reported resolution of each protein structure determination, are given in Table 9. We have generally chosen to only list the structural parameters reported in the original literature reports in Table 9. (A few exceptions were calculated from the coordinates reported in the Protein Data Bank; these values are clearly indicated.)

A comparison of the structural data for the protein derivatives given in Table 9 with those of the analogous iron derivatives given in the preceding sections clearly shows an issue that must be addressed. The geometrical descriptions of the FeNO group of analogous protein systems display significant variation, while the small molecule species are seen to have relatively narrow ranges for these values. For example, the Fe−N(NO) distances in the $\{FeNO\}^7$ and $\{FeNO\}^6$ derivatives each fall within a very narrow range, but the protein derivatives apparently display a larger range of values. Are the protein observations all correct and the result of the influence of the protein environment or other factors exclusive to the proteins? We think that scenario is quite unlikely as some values appear quite unlikely. We believe that the difficulties of multiple protein conformers and unrecognized disorder contribute to the problems of precisely defining the coordination group geometry. The report of four myoglobin derivatives at near-atomic resolution provides an instructive lesson about problems in protein structure determination.[99] In our view, the disorder problems outlined in that report are likely to be more general than has been recognized. Such disorder would clearly affect both Fe−N−O angles and Fe−N dis-

tances. In addition, for a variety of historical and experimental reasons, the quality of the protein structure analyses are quite uneven. Early structure determinations were carried out quite differently than recent work. Recent advances in data collection and refinement methods have led to structures of enhanced resolution and refinement of structural models. In the end, we have concluded that the most judicious approach would be to hold our comments to a minimum, to avoid trying to judge the merits of each structure determination, and to comment principally on the aggregate structural data set.

A. {FeNO}^{7} Proteins

The structures of a number of NO heme proteins whose function is the binding of dioxygen have been studied and are the first of the derivatives to be considered. The earliest reported structure is the iron(II)−(nitrosyl)hemoglobin complex (horse) reported by Deatherage and Moffat[100] that was resolved by difference Fourier analysis. NO binds on the distal side of the porphyrin (as does dioxygen). The α and β subunits of hemoglobin display two distinct nitrosyl heme complexes. The Fe−N−O bond lengths and angles are identical for both subunit types, although they differ in the relative orientation of the nitrosyl with respect to the Fe−N_p bonds of the porphyrin plane. The angles between the Fe−N−O plane and the Fe−N_p bond of pyrrole IV are 205 and 195° for the α and β subunits, respectively. The Fe−N−O angle of 145° for both systems is reasonable and corresponds well to the values observed for the iron(II) model complexes (Tables 2 and 3). This analysis of the difference Fourier maps suggests that the NO ligand heme stereochemistry is affected little by the protein environment. Comparison of the positions of the proximal histidine for both α and β subunits relative to their positions in the MetHb complex shows that for the α subunit, the proximal histidine and associated residues move away from the heme upon coordination of the nitrosyl. In the β subunit, however, coordination of nitric oxide causes the proximal histidine and associated F-helix to move closer to the heme plane. This leads to an assignment of five coordination for the α subunit heme and six coordination for the β subunit heme.

Structural studies on T-state (nitrosyl)hemoglobin (human)[101] clearly show the breaking of the Fe-proximal histidine bond upon coordination of NO in the α subunit, while the heme in the β subunit is six coordinate. This is in agreement with the Perutz cooperativity model[102] in that ligand-induced proximal stress in the α subunits of hemoglobin can lead to five-coordinate complexes. In the α subunit, the deoxyHbA system is found to contain an iron atom displaced 0.69 Å out-of-plane on the proximal side. Correspondingly, the T-state (nitrosyl)HbA complex contains an iron atom displacement of 0.26 Å toward the distal side. Thus, coordination of the nitrosyl ligand results in a 0.95 Å movement of the iron through the heme plane. By comparison, the iron moves only 0.4 Å for the β subunit, which also contains a more planar heme. In these systems, the Fe−N−O unit is again bent at 150 and 155°, respectively. Such structural variation is also consistent with the {FeNO}^{7} structural trans effect noted earlier.

A further (nitrosyl)hemoglobin system characterized is an S-nitroso hemoglobin derivative.[103] The protein is nitrosylated at Cys93β. Again, a bent Fe−N−O unit is observed, although the angles are smaller than typically observed in small molecule systems (131 and 123°, respectively). The increased bending is explained as being caused by either increased π bonding between the Fe and the nitrosyl ligand or electrostatic interactions between the nitrosyl and distal histidine. Aside from the unusually small bond angle, the only other feature of note is the fact that the hemes in both the α and β subunits appear to be six coordinate. This is somewhat puzzling since the major change in the tertiary protein structure appears only in the β subunit.

Studies have also been carried out on the nitrosyl complex of monomeric leghemoglobin.[104] The heme is found to be six-coordinate with histidine in the sixth position. The Fe−N(histidine) bond is long at 2.20 Å, a distance comparable to that in the few six-coordinate iron(II) model complexes (Table 3). The Fe−N−O bond angle of 147° is also reasonable.

A six-coordinate species is also observed for the nitrosyl complex of sperm whale myoglobin.[105] The long Fe−N(histidine) bond length might be evidence of the strong trans effect of NO, but the distance is no longer than that observed in some CO and O_2 structures. However, it is longer than the 2.06 Å distances seen in the recent near-atomic resolution structures of CO- and O_2-myoglobin.[99] The Fe−N−O bond angle is notably smaller than those of the model compounds at 112°. This angle is comparable to an estimate made for nitrosyl hemoglobin from a single-crystal EPR study.[106] The small value of this angle in (nitrosyl)Mb was rationalized in terms of electrostatic and proximal interactions, especially those of the distal histidine. The nitrogen of the distal histidine is 2.8 Å from the nitrosyl nitrogen and 3.4 Å from the oxygen. This compares to (nitrosyl)leghemoglobin where the distal histidine is at least 3.3 Å from both atoms; the FeNO group possesses a more "normal" Fe−N−O angle of 145°. Additional evidence for a possible electrostatic effect is provided by the structure of a mutant (nitrosyl)myoglobin complex.[107] Here, the pocket of the enzyme is less crowded; the complex is in the more loosely packed space group P6, and the Fe−N−O angle is found to be 130°.

A similarly small Fe−N−O angle of 112° is observed for the (nitrosyl)SHP complex from *Rhodobacter sphaeroides*.[108] This cytochrome *c* type protein is found to possess an unusual asparagine residue on the proximal side that swings away upon coordination of the nitrosyl. The small angle was explained by close contacts with a distal tryptophan residue located ~3.1 Å from the oxygen of the nitrosyl ligand.

Relatively small Fe−N−O angles are also observed for a microbial cytochrome *c*′ complex.[109] The most remarkable feature of this species is not simply the five-coordinate nature of the derivative but that NO has displaced the proximal histidine ligand; this feature is not observed in the CO adduct, which forms

the expected six-coordinate, histidine-ligated species. This unexpected coordination feature emphasizes a possible biological distinction between NO and CO as gaseous ligands, especially with respect to the gas-sensing hemoproteins. The nitrosyl ligand is found to be disordered over two equally occupied positions with Fe−N−O angles of 124 and 132°, respectively. These also differ in that one orientation forms a close contact—, a hydrogen bond with an arginine side chain within the pocket, while the other does not. This makes the equal occupancy of the two orientations surprising. Fe−N(NO) bond lengths for the nitrosyl complexes are longer than expected compared to the average value of 1.7 Å for the model complexes, although several other protein structures are also found to possess apparently long Fe−N(NO) bonds (Table 9).

Other heme proteins that have been structurally characterized with an NO ligand and their reported structural parameters are given in Table 9. These include the NO derivative of endothelial nitric oxide synthase both in the presence and in the absence of the tetrahydrobiopterin cofactor.[110] Two different cd_1 nitrite reductase derivatives have been reported: one from *Pseudomonas aeruginosa*[111] and a second from *Paracoccus denitrificans* known alternatively as *Thiophaera pantotropha*.[112] The site of NO binding is at the d_1 heme. Despite the similarities in structural parameters for the two cd_1 systems, different formal oxidation states were assigned;[111,112] in our opinion, the assignment as iron(II) ({FeNO}^{7}) appears to be more likely. The nitrosyl derivatives of cytochrome *c* peroxidase[113] and a siroheme class of nitrite reductase[114] are both six-coordinate species, although only the latter species shows a significant structural trans effect. The siroheme species has an unusual trans ligand: a thiolate sulfur from a bridging cysteine (bridges to an Fe_4S_4 cluster).

B. {FeNO}^{6} Proteins

Although the reaction of nitric oxide with a heme protein generally reduces an accessible iron(III) center to an iron(II) center, there are some heme proteins that have a clear physiological function as iron(III) centers. Prime examples include the NO carriers of blood-sucking insects and P450nor, a nitric oxide reductase from denitrifying fungi. The nitric oxide carriers from the blood-sucking insect *Rhodnius prolixus* (a member of the kissing bug family) are known as nitrophorins; these have been intensively studied.[115] The four nitrophorin isoforms carry NO in the insect's saliva, which acts as a vasodilator on their blood meal host. The nitrophorin iron(III) center must resist reduction by NO in order to function as an NO carrier.

The first attempt to structurally characterize a (nitrosyl)iron(III) form of a nitrophorin was made with isoform 1.[116] The NO derivative of NP1 was apparently photoreduced in the X-ray beam during data collection, and the values for this structure determination are appropriately reported in the {FeNO}^{7} section. The crystal structure of the (nitrosyl)nitrophorin 4 complex has subsequently been reported and is the first example of a protein structure containing an NO ligand coordinated to an iron(III) heme.[117] The challenge of the preparation of a (nitrosyl)iron(III) system was solved in part by flash-freezing crystals. The Fe−N−O unit is approximately linear (177°), although the Fe−N(NO) bond appears to be shorter than expected. A second orientation of the nitrosyl ligand is also observed with an Fe−N−O angle of 110°; this is probably from a ferrous impurity. The protein is observed to have an open distal pocket that closes upon the binding of NO; the binding of NO leads to a hydrophobic pocket around the NO. The heme is also noted to undergo substantial ruffling upon binding NO. A similar photoreduction in the X-ray beam has likely occurred in the crystal structures of three threonine mutants of P450nor; calculated values of the geometry around heme are only consistent with iron(II) species.[118]

One other ferric system has been structurally characterized, the nitrosyl adduct of soybean leghemoglobin, done by multiple scattering XAFS.[119] A structure for the iron(II) system has also been obtained. To interpret the data, the N−O bond length is fixed at 1.12 Å on the basis of existing model complexes. This yields data for the remainder of the Fe−N−O moiety that is also comparable to that observed for the model complexes. The most unusual feature observed is that the trans Fe−N(histidine) bond lengths are shorter than expected (1.98 Å for iron(II) and 1.89 Å for iron(III)).

C. Nitrite Binding Proteins

There are a number of protein systems that are known to reduce nitrite (nitrite reductases). There are four categories of such systems known to us, and three contain a heme prosthetic group that binds nitrite ion. The one system that does not contain heme centers contains copper (class I) and will not be considered. The three heme-containing systems are: (i) the class II reductases that contain two hemes (the cd_1 family), (ii) the class III reductases that contain multiple hemes, and (III) the siroheme reductase systems that also reduce sulfite. General overviews of denitrification cycles and possible mechanisms for the conversion of nitrite have been considered in two reviews.[1,120]

Members of the cd_1 family have a noncovalently linked d_1 heme site that is the site of reduction of nitrite. For the cd_1 systems, nitrite is reduced to nitric oxide. One crystal structure for a nitrite-bound cd_1 system is available. The structure was determined from a freeze-quenched crystal of the reductase from *T. pantotropha*.[112] The nitrite is bound to the d_1 heme in subunit A of the protein. The nitrite is coordinated via nitrogen in a nitro form; both oxygen atoms of the nitrite are found to be positioned suitably for hydrogen bonding to neighboring histidine residues. This agrees with the idea that these histidines provide the protons to a nitrite oxygen atom that forms a water molecule.

The other nitrite reductases catalyze the reduction of nitrite to ammonia in a six-electron process; the potential intermediates NO and hydroxylamine are not released during nitrite turnover. The multiheme nitrite reductases are termed cytochrome *c* nitrite

reductases. Einsle et al.[121] have determined the crystal structure of the enzyme isolated from the microorganism *Sulfurospirillum deleyianum*. The protein is a homodimer with five hemes per monomer. The active site is a noncovalently linked, high-spin iron protoporphyrin IX derivative that has the unusual amino acid lysine as the fifth ligand. This site is known to bind nitrite through the nitrogen atom.[122] Einsle et al. have also noted that the closely packed arrangement of hemes that they observed for cytochrome *c* nitrite reductase was very similar to that seen in the enzyme hydroxylamine oxidoreductase,[123] even though the functions of the two enzymes are very different. Both the cytochrome *c* nitrite reductases and hydroxylamine oxidoreductase do have an electron transport chain requirement, and most of the hemes are involved in that chain.

The crystal structures of several different derivatives of sulfite reductase, which also catalyzes the reduction of nitrite in a similar six-electron process, have been determined.[114] This class of (plant) sulfite and nitrate reductases contain a siroheme (a tetrahydroporphyrin of the isobacteriochlorin class) bridged to an Fe_4S_4 cluster; the sixth coordination site is the expected site of catalytic activity. In the nitrite derivative, the nitrite ligand is coordinated via the nitrogen atom to the iron atom of the siroheme. The porphyrin is very slightly domed with the iron of the heme being displaced 0.08 Å above the heme plane. The oxygen atoms of the nitrite are within hydrogen bonding distance of nearby arginine and lysine residues of the protein, a source for protons for the conversion of nitrite to water and nitric oxide in the first steps of the conversion of nitrite to ammonia.

A number of factors in the crystallization of protein derivatives, the difficulties of coordinating the desired ligand to the active site while preventing other reactions, and the poorer resolution will always limit the quality of protein structures. Despite these problems, a number of heme protein structures containing coordinated nitrosyl ligands have been obtained. Although there is far larger variation in the bond lengths and angles observed for the proteins (all iron species) than for the analogous iron(II) and iron(III) porphyrinate derivatives, similar trends are observed. The constraints of the protein appear to be important in defining whether five- or six-coordinate iron(II)nitrosyl species are obtained. The formation of five-coordinate nitrosyl species as a result of the structural trans effect appears to be largely limited to the oxygen-carrying derivatives, nitric oxide synthase, and guanylate cyclase. A possible explanation is that the protein structure provides sufficient rigidity on the proximal side to keep the proximal ligand within coordinating distance of the iron atom. Importantly, the apparently wide variation in coordination group geometry of the heme protein derivatives, if real, should lead to observable differences in spectroscopic properties, especially vibrational features associated with the FeNO group. Finally, protein derivatives with coordinated nitrite also appear to be closely similar to those of the analogous small molecule structures.

V. Summary

The tables given in the text have summarized the salient stereochemical features of the small molecule metalloporphyrin derivatives with nitric oxide, nitrite, and nitrate as axial ligands. The data tabulated therein clearly show that there are structural expectation values for each metal ion, its oxidation level, and axial ligand. Some possible nuances are also apparent. The unequaled variety displayed by the iron derivatives, commensurate with their biological functions, is clear and consistent with their heme protein role as redox catalysts and gas carriers/sensors. Iron derivatives alone significantly utilize more than one oxidation state and display a variety of structural types.

VI. Acknowledgments

W.R.S. gratefully acknowledges the U.S. National Institutes of Health (Grant GM-38401) for its long-term support of his metalloporphyrin research program. We also thank Dr. Mary Ellison for discussion and assistance.

VII. Abbreviations

A. Porphyrins and Ligands

18-C-6	18-crown-6 (1,4,7,10,13,16-hexaoxacyclooctadecane)
p-C_6H_5F	*para*-fluorophenyl anion
Cl_2Py	2,6-dichloropyridine
Ct	center of the 24 atom porphyrin core
HIm	imidazole
Iz	indazole (benzopyrazole)
3,5-Lut	3,5-dimethylpyridine
1-MeIm	1-methylimidazole
4-MePip	4-methylpiperidine
N_p	porphyrinato nitrogen
(O-*n*-Bu)	*n*-butoxide anion
OC_2OPor	dianion of 5,10,15,20-tetrakis(2-phenyloxy)-ethoxy-2′,2″,2‴,2⁗-tetraarylporphyrin
OECorrole	trianion of octaethylcorrole
OEP	dianion of octaethylporphyrin
OEP′	dianion of *trans*-21,22-bis(ethoxycarbonylmethyl)octaethylporphyrin
OEP-*t*-Bu_2	dianion of 5,15-*tert*-butyloctaethylporphodimethene
(O_2PF_2)	difluorophosphate anion
OETAP	dianion of octaethyltetraazaporphyrin
OEt	ethoxide anion
oxoOEC	dianion of oxooctaethylchlorin(2-oxo-3,3′,7,8,-12,13,17,18-octaethylporphyrin)
Pip	piperidine
PMS	pentamethylene sulfide
Por	a generalized porphyrin dianion
Prz	pyrazine
Py	pyridine
Pz	pyrazole
S-C_6HF_4	2,3,5,6-tetrafluorothiophenolate
S-NACysMe	*S*-nitroso-*N*-acetyl-L-cysteine methyl ester
T2,6-Cl_2PP	dianion of *meso*-tetra-2,6-dichlorophenylporphyrin
Tp-OCH_3PP	dianion of *meso*-tetra-*p*-methoxyphenylporphyrin
TpivPP	dianion of *meso*-α,α,α,α-tetrakis(*o*-pivalamidophenyl)porphyrin
TPP	dianion of *meso*-tetraphenylporphyrin

$TPPBr_4$	dianion of 7,8,17,18-tetrabromo-*meso*-tetraphenylporphyrin
$TPPBr_8$	dianion of 2,3,7,8,12,13,17,18-octabromo-*meso*-tetraphenylporphyrin
$TPPBr_4NO_2$	dianion of 2-nitro-7,8,17,18-tetrabromo-*meso*-tetraphenylporphyrin
TTP	dianion of *meso*-tetratolylporphyrin

B. Proteins

CCP	yeast cytochrome *c* peroxidase
cd_1-NIR(*pa*)	cytochrome cd_1 nitritereductase from *Pseudomonas aeruginosa*
cd_1-NIR(*tp*)	cytochrome cd_1 nitritereductase from *Thiosphaera pantotropha*
cyt c'	cytochrome c' from *Alcaligenes xylosoxidons*
4HB	cofactor tetrahydrobiopterin
α-Hb	nitrosylated horse hemoglobin, α subunit
β-Hb	nitrosylated horse hemoglobin, β subunit
α-T-Hb_A	T-state human hemoglobin A, α subunit
β-T-Hb_A	T-state human hemoglobin A, β subunit
Lupin-Lb^{II}	Lupin ferrous leghemoglobin
Mb	Sperm Whale myoglobin
L29F-Mb	mutant (L29F) Sperm Whale myoglobin
NOS	bovine endothelial nitric oxide synthase
NP1	nitrophorin 1 from *Rhodnius prolixus* saliva
NP4	nitrophorin 4 from *Rhodnius prolixus* saliva
SHP	sphaeroides heme protein from *Rhodobacter sphaeroides*
SiRHP	sulfite reductase heme protein from *Escherichia coli*
α-SNO-nitrosylHbA	S-nitroso form of human hemoglobin, α subunit
β-SNO-nitrosylHbA	S-nitroso form of human hemoglobin, β subunit
soybean-Lb^{II}	soybean ferrous leghemoglobin A
soybean-Lb^{III}	soybean ferric leghemoglobin A
T243A-P450nor	mutant (T243A) cytochrome P450nor (fungal nitric oxide reductase)
T243N-P450nor	mutant (T243N) cytochrome P450nor (fungal nitricoxide reductase)
T243V-P450nor	mutant (T243V) cytochrome P450nor (fungal nitricoxide reductase)

VIII. References

(1) Averill, B. A. *Chem. Rev.* **1996**, *96*, 2951.
(2) Butler, A. R.; Williams, D. L. H. *Chem. Soc. Rev.* **1993**, 233.
(3) Bredt, D. S.; Snyder, S. H. *Annu. Rev. Biochem.* **1994**, *63*, 175.
(4) Schmidt, H. H.; Walter, U. *Cell* **1994**, *78*, 919.
(5) Ribiero, J. M. C.; Hazzard, J. M. H.; Nussenzveig, R. H.; Champagne, D. E.; Walker, F. A. *Science* **1993**, *260*, 539.
(6) Feltham, R. D.; Enemark, J. H. *Top. Stereochem.* **1981**, *12*, 155.
(7) Scheidt, W. R.; Ellison, M. K. *Acc. Chem. Res.* **1999**, *32*, 2. 350.
(8) Cheng, L.; Richter-Addo, G. B. In *The Porphyrin Handbook*; Kadish, K. M., Smith, K. M.; Guilard, R., Eds.; Academic Press: New York, 2000; Vol. 4, pp 219−291.
(9) Richter-Addo, G. B.; Legzdins, P. *Metal Nitrosyls*; Oxford University Press: New York, 1992.
(10) We explicitly will not include phthalocyanine species. To our knowledge, this only excludes complexes with nitrite and nitrate ligands.
(11) (a) Enemark, J. H.; Feltham, R. D. *Coord. Chem. Rev.* **1974**, 13, 339. (b) Updated by Enemark in Westcott, B. L.; Enemark, J. H. In *Inorganic Electronic Structure and Spectroscopy*; Lever, A. B. P., Solomon, E. I., Eds.; Wiley-Interscience Publications: New York, 1999; Vol. 2, pp 403−450.
(12) Coppens, P.; Novozhilova, I.; Kovalevsky, A. *Chem. Rev.* **2002**, *102*, 861−884|
(13) Scheidt, W. R.; Hoard, J. L. *J. Am. Chem. Soc.* **1973**, *95*, 8281.
(14) Groombridge, C. J.; Larkworthy, L. F.; Mason, J. *Inorg. Chem.* **1993**, *32*, 379.
(15) Richter-Addo, G. B.; Hodge, S. J.; Yi, G.-B.; Khan, M. A.; Ma, T.; Caemelbecke, E. V.; Guo, N.; Kadish, K. M. *Inorg. Chem.* **1996**, *35*, 6350. Correction: Richter-Addo, G. B.; Hodge, S. J.; Yi, G.-B.; Khan, M. A.; Ma, T.; Caemelbecke, E. V.; Guo, N.; Kadish, K. M. *Inorg. Chem.* **1997**, *36*, 2696.
(16) Ellison, M. K.; Scheidt, W. R. *Inorg. Chem.* **1998**, *37*, 382.
(17) Godbout, N.; Sanders, L. K.; Salzmann, R.; Havlin, R. H.; Wojdelski, M.; Oldfield, E. *J. Am. Chem. Soc.* **1999**, *121*, 3829.
(18) Scheidt, W. R. Unpublished results.
(19) Kadish, K. M.; Ou, Z.; Tan, X.; Boschi, T.; Monti, D.; Fares, V.; Tagliesti, P. *J. Chem. Soc., Dalton Trans.* **1999**, 1595.
(20) Jene, P. G.; Ibers, J. A. *Inorg. Chem.* **2000**, *39*, 5796.
(21) Scheidt, W. R.; Hatano, K.; Rupprecht, G. A.; Piciulo, P. L. *Inorg. Chem.* **1979**, *18*, 292.
(22) Piciulo, P. G.; Rupprecht, G.; Scheidt, W. R. *J. Am. Chem. Soc.* **1974**, *96*, 5293.
(23) Diebold, T.; Schappacher, M.; Chevrier, B.; Weiss, R. *J. Chem. Soc., Chem. Commun.* **1979**, 693.
(24) Colin, J.; Strich, A.; Schappacher, M.; Chevrier, B.; Veillard, A.; Weiss, R. *Nouv. J. Chem.* **1994**, *8*, 55.
(25) Scheidt, W. R.; Frisse, M. E. *J. Am. Chem. Soc.* **1975**, *97*, 17.
(26) Ellison, M. K.; Scheidt, W. R. *J. Am. Chem. Soc.* **1997**, *119*, 7404.
(27) Scheidt, W. R.; Duval, H. F.; Neal, T. J.; Ellison, M. K. *J. Am. Chem. Soc.* **2000**, *122*, 4651.
(28) Bohle, D. S.; Debrunner, P.; Fitzgerald, J. P.; Hansert, B.; Hung, C.-H.; Thomson, A. J. *J. Chem. Soc., Chem. Commun.* **1997**, 91.
(29) Nasri, H.; Haller, K. J.; Wang, Y.; Hunyh, B. H.; Scheidt, W. R. *Inorg. Chem.* **1992**, *31*, 3459.
(30) Cheng, L.; Powell, D. R.; Khan, M. A.; Richter-Addo, G. B. *J. Chem. Soc., Chem. Commun.* **2000**, 2301.
(31) Bohle, D. S.; Hung, C.-H. *J. Am. Chem. Soc.* **1995**, *117*, 9584.
(32) Scheidt, W. R.; Reed, C. A. *Chem. Rev.* **1981**, *81*, 543.
(33) Scheidt, W. R.; Lee, Y. J. *Struct. Bonding (Berlin)* **1987**, *64*, 1−70.
(34) Ghosh, A.; Wondimagegn, T. *J. Am. Chem. Soc.* **2000**, *122*, 8101.
(35) Cheng, L.; Novozhilova, I.; Kim, C.; Kovalevsky, A.; Bagley, K. A.; Coppens, P.; Richter-Addo, G. B. *J. Am. Chem. Soc.* **2000**, *122*, 7142.
(36) Scheidt, W. R.; Piciulo, P. L. *J. Am. Chem. Soc.* **1976**, *98*, 1913.
(37) Safo, M. K.; Scheidt, W. R.; Gupta, G. P. *Inorg. Chem.* **1990**, *29*, 626.
(38) Scheidt, W. R.; Brinegar, A. C.; Ferro, E. B.; Kirner, J. F. *J. Am. Chem. Soc.* **1977**, *99*, 7315.
(39) The value of the Fe−N(Pip) bond distance in $[Fe(TPP)(Pip)_2]$ is 2.127(3) Å. See: Radonovich, L. J.; Bloom, A.; Hoard, J. L. *J. Am. Chem. Soc.* **1972**, *94*, 2073.
(40) Wyllie, G. R. A.; Scheidt, W. R. Work in progress.
(41) Kon, H.; Kataoka, N. *Biochemistry* **1969**, *8*, 4757.
(42) Wayland, B. B.; Minkiewicz, J. V.; Abd-Elmageed, M. E. *J. Am. Chem. Soc.* **1974**, *96*, 2795.
(43) (a) Dierks, E. A.; Hu, S.; Vogel, K. M.; Yu, A. E.; Spiro, T. G.; Burstyn, J. N. *J. Am. Chem. Soc.* **1997**, *119*, 7316. (b) Deinum, G.; Stone, J. R.; Babcock, G. T.; Marletta, M. A. *Biochemistry* **1996**, *35*, 1540.
(44) Stone, J. R.; Marletta, M. *Biochemistry* **1994**, *33*, 5636.
(45) Maxwell, J. C.; Caughey, W. S. *Biochemistry* **1976**, *15*, 388.
(46) Szabo, A.; Barron, L. D. *J. Am. Chem. Soc.* **1975**, *97*, 660. Szabo, A.; Perutz, M. F. *Biochemistry* **1976**, *15*, 4427.
(47) Yonetani, T.; Tsuneshige, A.; Zhou, Y.; Chen, X. *J. Biol. Chem.* **1998**, *273*, 20323.
(48) Nasri, H.; Wang, Y.; Huynh, B. H.; Scheidt, W. R. *J. Am. Chem. Soc.* **1991**, *113*, 717.
(49) Nasri, H.; Ellison, M. K.; Chen, S.; Hunyh, B. H.; Scheidt, W. R. *J. Am. Chem. Soc.* **1997**, *119*, 6274.
(50) Scheidt, W. R.; Lee, Y. J.; Hatano, K. *J. Am. Chem. Soc.* **1984**, *106*, 3191.
(51) Ellison, M. K.; Schulz, C. E.; Scheidt, W. R. *Inorg. Chem.* **2000**, *39*, 5102.
(52) Autret, M.; Will, S.; Caemelbecke, E. V.; Lex, J.; Gisselbrecht, J.-P.; Gross, M.; Vogel, E.; Kadish, K. M. *J. Am. Chem. Soc.* **1994**, *116*, 9141.
(53) Yi, G.-B.; Chen, L.; Khan, M. A.; Richter-Addo, G. B. *Inorg. Chem.* **1997**, *36*, 3876.
(54) Ellison, M. K.; Scheidt, W. R. *J. Am. Chem. Soc.* **1999**, *121*, 5210.
(55) Ellison, M. K.; Schulz, C. E.; Scheidt, W. R. *Inorg. Chem.* **1999**, *38*, 100.
(56) Richter-Addo, G B.; Wheeler, R. A.; Hixson, C. A.; Chen, L.; Khan, M. A.; Ellison, M. K.; Schulz, C. E.; Scheidt, W. R. *J. Am. Chem. Soc.* **2001**, *123*, 6314.
(57) (a) Gibson, Q. H.; Roughton, F. J. W. *Proc. R. Soc. London, Ser. B* **1957**, *147*, 44. (b) Gibson, Q. H.; Roughton, F. J. W. *Proc. R. Soc. London, Ser. B* **1965**, *163*, 197. (c) Traylor, T. G.; Sharma, V. S. *Biochemistry* **1992**, *31*, 2847.

(58) (a) Hoshino, M.; Ozawa, K.; Seki, H.; Ford, P. C.; *J. Am. Chem. Soc.* **1993**, *115*, 9568. (b) Laverman, L. E.; Wanat, A.; Oszajca, J.; Stochel, J.; Ford, P. C.; van Eldik, R. *J. Am. Chem. Soc.* **2001**, *123*, 285.
(59) Guilard, R.; Boisselier-Cocolios, B.; Tabard, A.; Cocolios, P.; Simonet, B.; Kadish, K. M. *Inorg. Chem.* **1985**, *24*, 2509.
(60) Ellison, M. K. Ph.D. Thesis, University of Notre Dame, Notre Dame, IN, 2001.
(61) Lin, R.; Farmer, P. J. *J. Am. Chem. Soc.* **2001**, *123*, 1143.
(62) Lorkovic, I. M.; Ford, P. C. *Inorg. Chem.* **2000**, *39*, 632.
(63) Kadish, K. M.; Adamian, V. A.; Caemelbacke, E. V.; Tan, Z.; Tagliesta, P.; Bianco, P.; Boschi, T.; Yi, G.-B.; Khan, M. A.; Richter-Addo, G. B. *Inorg. Chem.* **1996**, *35*, 1343.
(64) Bohle, D. S.; Goodson, P. G.; Smith, B. D. *Polyhedron* **1996**, *15*, 3147.
(65) Yi, G.-B.; Khan, M. A.; Richter-Addo, G. B. *Inorg. Chem.* **1996**, *35*, 3453.
(66) Yi, G.-B.; Khan, M. A.; Richter-Addo, G. B. *J. Chem. Soc., Chem. Commun.* **1996**, 2045.
(67) Bohle, D. S.; Hung, C.-H.; Powell, A. K.; Smith, B. D.; Wocaldo, S. *Inorg. Chem.* **1997**, *36*, 1992.
(68) Yi, G.-B.; Khan, M. A.; Powell, D. R.; Richter-Addo, G. B. *Inorg. Chem.* **1998**, *37*, 208.
(69) Miranda, K. M.; Bu, X.; Lorkovic, I.; Ford, P. C. *Inorg. Chem.* **1997**, *36*, 4838.
(70) Chen, L.; Yi, G.-B.; Wang, L.-S.; Dharmawardana, U. R.; Dart, A. C.; Khan, M. A.; Richter-Addo, G. B. *Inorg. Chem.* **1998**, *37*, 4677.
(71) Bohle, D. S.; Hung, C.-H.; Smith, B. D. *Inorg. Chem.* **1998**, *37*, 5798.
(72) Hodge, S. J.; Wang, L.-S.; Khan, M. A.; Young, V. G.; Richter-Addo, G. B. *J. Chem. Soc., Chem. Commun.* **1996**, 2283.
(73) Leung, W.-H.; Chim, J. L. C.; Lai, W.; Lam, L.; Wong, W.-T.; Chan, W. H.; Yeung, C.-H. *Inorg. Chim. Acta* **1999**, *290*, 28.
(74) Byrn, M. P.; Curtis, C. J.; Khan, S. I.; Sawin, P. A.; Tsurumi, R.; Strouse, C. *J. Am. Chem. Soc.* **1990**, *112*, 1865.
(75) Cheng, L.; Chen, L.; Chung, H. S.; Khan, M. A.; Richter-Addo, G. B.; Young, V. G. *Organometallics* **1998**, *17*, 3853.
(76) Chen, L.; Khan, M. A.; Richter-Addo, G. B. *Inorg. Chem.* **1998**, *37*, 533.
(77) Cheng, L.; Powell, D. R.; Khan, M. A.; Richter-Addo, G. B. *Inorg. Chem.* **2001**, *40*, 125.
(78) Finnegan, M. G.; Lappin, A. G.; Scheidt, W. R. *Inorg. Chem.* **1990**, *29*, 181.
(79) Nasri, H.; Goodwin, J. A.; Scheidt, W. R. *Inorg. Chem.* **1990**, *29*, 185.
(80) Nasri, H.; Wang, Y.; Huynh, B. H.; Walker, F. A.; Scheidt, W. R. *Inorg. Chem.* **1991**, *30*, 1483.
(81) Nasri, H.; Scheidt, W. R.; Huynh, B. H.; Lloyd, S. G. Unpublished results.
(82) Nasri, H.; Ellison, M. K.; Krebs, C.; Huynh, B. H.; Scheidt, W. R. *J. Am. Chem. Soc.* **2000**, *122*, 10795.
(83) Jene, P. G.; Ibers, J. A. *Inorg. Chem.* **2000**, *39*, 3823.
(84) Kaduk, J. A.; Scheidt, W. R. *Inorg. Chem.* **1974**, *13*, 1875.
(85) Yamamoto, K.; Iitaka, Y. *Chem. Lett.* **1989**, 697.
(86) Goodwin, J.; Bailey, R.; Pennington, W.; Rasberry, R.; Green, T.; Shasho, S.; Echevarria, V.; Tiedeken, J.; Brown, C.; Fromm, G.; Lyerly, S.; Watson, N.; Long, A.; De Nitto, N.; *Inorg. Chem.* **2001**, *40*, 4217.
(87) Suslick, K. S.; Watson, R. A. *Inorg. Chem.* **1991**, *30*, 912.
(88) Ellison, M. K.; Shang, M.; Kim, J.; Scheidt, W. R. *Acta Crystallogr., Sect. C* **1996**, *C52*, 3040.
(89) Munro, O. Q.; Scheidt, W. R. Unpublished results.
(90) Phillippi, M. A.; Baenziger, N.; Goff, H. M. *Inorg. Chem.* **1981**, *20*, 3904.
(91) Munro, O. Q.; Scheidt, W. R. *Inorg. Chem.* **1998**, *37*, 2308.
(92) Okubo, Y.; Okamura, A.; Imanishi, K.; Tachibana, J.; Umakoshi, K.; Sasaki, Y.; Imamura, T. *Bull. Chem. Soc. Jpn.* **1999**, *72*, 2241.
(93) Batten, P.; Hamilton, A. L.; Johnson, A. W.; Mahendran, M.; Ward, D.; King, T. J. *J. Chem. Soc., Perkin Trans. 1* **1977**, 1623.
(94) Wyllie, G. R. A.; Munro, O. Q.; Schulz, C. E.; Scheidt, W. R. Work in progress.
(95) Nasri, H.; Turoska-Tyrk, I.; Scheidt, W. R. Unpublished results.
(96) Nasri, H.; Scheidt, W. R. Unpublished results.
(97) Eich, R. F.; Li, T.; Lemon, D. D.; Doherty, D. H.; Curry, S. R.; Aitken, J. F.; Mathews, A. J.; Johnson, K. A.; Smith, R. D.; Phillips, G. N., Jr.; Olson, J. S. *Biochemistry* **1996**, *35*, 6796.
(98) Arnold, E. V.; Bohle, D. S. *Methods Enzymol.* **1996**, *269*, 41.
(99) Vojtechovsky, J.; Chu, K.; Berendzen, J.; Sweet, R. M.; Schlichting, I. *Biophys. J.* **1999**, *77*, 2153.
(100) Deatherage, J. F.; Moffat, K. *J. Mol. Biol.* **1979**, *134*, 401.
(101) Chan, N.-L. Ph.D. Dissertation, University of Iowa, Iowa City, IA, 1998.
(102) (a) Perutz, M. *Nature* **1970**, *228*, 726. (b) Perutz, M. *Nature* **1970**, *237*, 495.
(103) Chan, N.-L.; Rogers, P. H.; Arnone, A. *Biochemistry* **1998**, *37*, 16459.
(104) Harutyunyan, E. H.; Safonova, T. N.; Kuranova, I. P.; Popov, A. N.; Teplyakov, A. V.; Oblomova, G. V.; Vainshtein, B. K.; Dodson, G. G.; Wilson, J. C. *J. Mol. Biol.* **1996**, *264*, 152.
(105) Brucker, E. A.; Olson, J. S.; Ikeda-Saito, M.; Phillips, G. N., Jr. *Proteins: Struct., Funct., Genet.* **1998**, *30*, 352.
(106) Chien, J. C. W. *J. Chem. Phys.* **1969**, *51*, 4220.
(107) Brucker, E. A.; Phillips, G. N., Jr. Unpublished results reported in reference 105.
(108) Leys, D.; Backers, K.; Meyer, T. E.; Hagen, W. R.; Cusanovich, M. A.; Van Beeumen, J. J. *J. Biol. Chem.* **2000**, *275*, 16050.
(109) Lawson, D. M.; Stevenson, C. E. M.; Andrew, C. R.; Eady, R. R. *EMBO J.*, **2000**, *19*, 5661.
(110) Li, H.; Raman, C. S.; Martasek, P.; Masters, B. S. S.; Poulos, T. L. *Biochemistry* **2001**, *81*, 40.
(111) Nurizzo, D.; Cutruzzola, F.; Arese, M.; Bourgeois, D.; Brunori, M.; Cambillau, C.; Tegoni, M. *Biochemistry* **1998**, *37*, 13987.
(112) (a) Williams, P. A.; Fülöp, V.; Garman, E. G.; Saunders, N. F. W.; Ferguson, S. J.; Hajdu, J. *Nature* (London), **1997**, *389*, 406. (b) Fülöp, V.; Moir, J. W. B.; Ferguson, S. J.; Hajdu, J. *Cell* **1995**, *81*, 369.
(113) Edwards, S. L.; Poulos, T. L. *J. Biol. Chem.* **1990**, *265*, 2588.
(114) Crane, B. R.; Siegel, L. M.; Getzoff, E. D. *Biochemistry* **1997**, *36*, 12120.
(115) Walker, F. A.; Monfort, W. R. In *Advances in Inorganic Chemistry*; Sykes, A. G., Mauk, G., Eds.; Academic Press: San Diego, CA, 2000, pp 295−358.
(116) Ding, X. A.; Weichsel, A.; Anderson, J. F.; Shokhireva, T. Kh.; Balfour, C.; Pierik, A. J.; Averill, B. A.; Montfort, W. R.; Walker, F. A. *J. Am. Chem. Soc.* **1999**, *121*, 128.
(117) Weischel, A.; Anderson J. F.; Roberts, S. A.; Montfort, W. R. *Nat. Struct. Biol.* **2000**, *7*, 551.
(118) Obayashi, E.; Shimizu, H.; Park, S.-Y.; Shoun, H.; Shiro, Y. *J. Inorg. Biochem.* **2000**, *82*, 103.
(119) Rich, A. M.; Ellis, P. J.; Tennant, L.; Wright, P. E.; Armstrong, R. S.; Lay, P. A. *Biochemistry* **1999**, *38*, 16491.
(120) Wasser, I. M.; de Vries, S.; Moënne-Loccoz, P.; Schröder, I.; Karlin, K. M. *Chem. Rev.* **2002**, *102*, 1201−1234.
(121) Einsle, O.; Messerschmidt, A.; Stach, P.; Bourenkov, G. P.; Bartunik, H. D.; Huber, R.; Kroneck, P. M. H. *Nature* **1999**, *400*, 476. 122.
(122) Einsle, O.; Neese, F.; Messerschmidt, A.; Kroneck, P. M. H. Work in progress.
(123) Igarashi, N.; Moriyama, H.; Fujiwara, T.; Fukumori, Y.; Tanaka, N. *Nat. Struct. Biol.* **1997**, *4*, 276.

CR000080P